

^{99m}Tc-Cyclopentadienyl Tricarbonyl Chelate-Labeled Compounds as Selective Sigma-2 Receptor Ligands for Tumor Imaging

Dan Li,^{†,‡} Yuanyuan Chen,^{†,‡} Xia Wang,[†] Winnie Deuther-Conrad,[‡] Xin Chen,[†] Bing Jia,[§] Chengyan Dong,^{||} Jörg Steinbach,[‡] Peter Brust,[‡] Boli Liu,[†] and Hongmei Jia^{*,†}

[†]Key Laboratory of Radiopharmaceuticals (Beijing Normal University), Ministry of Education, College of Chemistry, Beijing Normal University, Beijing 100875, China

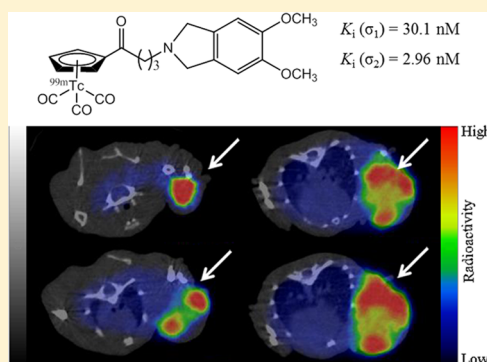
[‡]Institute of Radiopharmaceutical Cancer Research/Department of Neuroradiopharmaceuticals, Helmholtz-Zentrum Dresden-Rossendorf, 04318 Leipzig, Germany

[§]Medical and Healthy Analytical Center, Peking University, Beijing 100191, China

^{||}Interdisciplinary Laboratory, Institute of Biophysics, Chinese Academy of Sciences, Beijing 100101, China

S Supporting Information

ABSTRACT: We have designed and synthesized a series of cyclopentadienyl tricarbonyl rhenium complexes containing a 5,6-dimethoxyisoindoline or a 6,7-dimethoxy-1,2,3,4-tetrahydroisoquinoline pharmacophore as σ_2 receptor ligands. Rhenium compound **20a** possessed low nanomolar σ_2 receptor affinity ($K_i = 2.97$ nM) and moderate subtype selectivity (10-fold). Moreover, it showed high selectivity toward vesicular acetylcholine transporter (2374-fold), dopamine D_{2L} receptor, NMDA receptor, opiate receptor, dopamine transporter, norepinephrine transporter, and serotonin transporter. Its corresponding radiotracer [^{99m}Tc]**20b** showed high uptake in a time- and dose-dependent manner in DU145 prostate cells and C6 glioma cells. In addition, this tracer exhibited high tumor uptake (5.92% ID/g at 240 min) and high tumor/blood and tumor/muscle ratios (21 and 16 at 240 min, respectively) as well as specific binding to σ receptors in nude mice bearing C6 glioma xenografts. Small animal SPECT/CT imaging of [^{99m}Tc]**20b** in the C6 glioma xenograft model demonstrated a clear visualization of the tumor at 180 min after injection.



INTRODUCTION

Uncontrolled cell proliferation is one of the hallmarks of cancer, and its assessment will provide useful information to predict the tumor aggressiveness and prognosis of cancer.¹ The sigma-2 (σ_2) receptors are upregulated in a wide variety of human and rodent tumor cells.^{2–6} Moreover, they showed an approximately 10-fold higher expression in proliferating versus quiescent tumors.^{7–9} Significant effort has been dedicated to the validation of the σ_2 receptor as a biomarker for the imaging of the proliferative status of solid tumors.^{7–15} Currently, a promising radiotracer targeting σ_2 receptors, *N*-(4-(6,7-dimethoxy-3,4-dihydroisoquinolin-2(1*H*)-yl)butyl)-2-(2-[¹⁸F]fluoroethoxy)-5-methylbenzamide ([¹⁸F]ISO-1), is under clinical trials.^{10–12} Furthermore, a significant correlation between the uptake of this radiotracer and Ki-67 (the “gold standard” used in histological measurements of cell proliferation in tumor surgical and biopsy specimens) was observed in human studies.¹² These findings indicate that the σ_2 receptor is an important biomarker for determining the proliferative status of solid tumors using positron emission tomography (PET).^{13–15}

It is well-known that single photon emission computed tomography (SPECT) is an extremely helpful, widely used, and low cost clinical imaging modality. ^{99m}Tc is still the most widely

used radionuclide in clinical nuclear medicine application. With the clinical implementation of quantitative SPECT in the future,¹⁶ ^{99m}Tc-labeled radiotracers with high affinity, high selectivity, and specificity for σ_2 receptors will provide a unique tool for the early diagnosis of cancer and assessment of the proliferative status of solid tumors. Over the past few decades, a series of ^{99m}Tc-labeled radioligands targeting σ_2 receptors have been reported.^{17–22} However, there is a lack of ideal ^{99m}Tc-labeled radiotracers for imaging σ_2 receptors in human studies. Therefore, the development of ^{99m}Tc-labeled σ_2 receptor radioligands is very attractive.

Previously, our structure–affinity relationship analyses indicated the high importance of the σ_2 preferring group to improve the selectivity for σ_2 receptors.²³ Besides the 6,7-dimethoxy-1,2,3,4-tetrahydroisoquinoline scaffold in ISO-1, the 5,6-dimethoxyisoindoline moiety was identified as a promising σ_2 preferring group with less lipophilicity.²⁴ Moreover, the [(Cp-R)Tc(CO)₃] unit can be incorporated into selective receptor ligands without a significant change in the biological properties via an appropriate linker.^{22,25} In the present study, our aim is to

Received: September 5, 2015

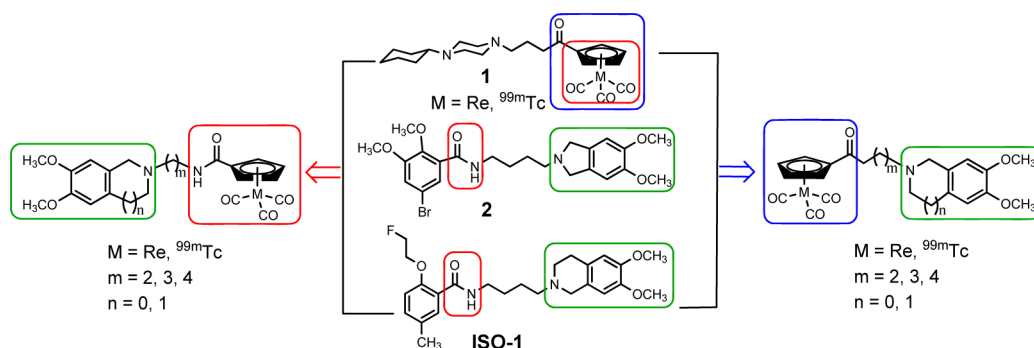
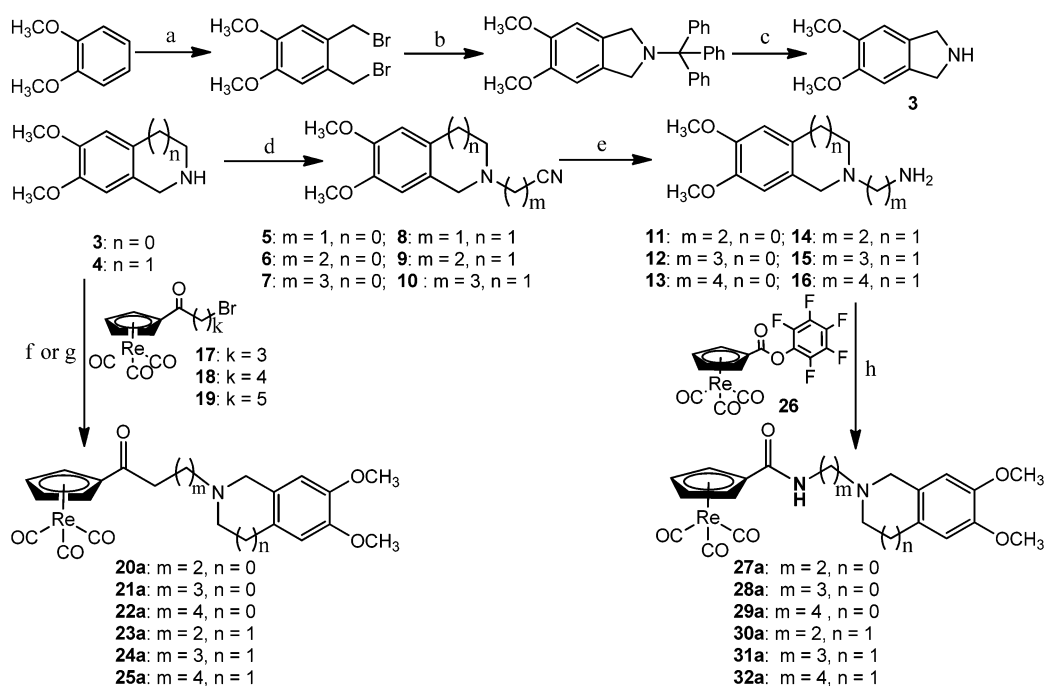


Figure 1. Design concept of novel $[(\text{Cp-R})\text{M}(\text{CO})_3]$ ($\text{M} = {}^{99\text{m}}\text{Tc}$, Re) complexes as potent σ_2 receptor ligands.

Scheme 1. Synthetic Routes of the Rhenium Compounds^a



^aReagents and conditions: (a) 33% HBr/HOAc, rt (20 h)–65 °C (1 h), 32%; (b) tritylamine, DIEA, DMF, 60 °C, 2 h, 77%; (c) TFA, $\text{CHCl}_3/\text{MeOH}$, 0 °C–rt, 1 h, 69%; (d) $\text{Br}(\text{CH}_2)_m\text{CN}$, Et_3N , CH_2Cl_2 , rt, 24 h, for 5–7, 67–73%, for 8–10, 59–70%; (e) LiAlH_4 , $\text{THF-Et}_2\text{O}$, 0 °C–rt, 24 h, for 11–13, 36–50%, for 14–16, 27–40%; (f) toluene, 3 or 4, KI , Et_3N , 115 °C, 10% for 20a, 10% for 21a, 30% for 23a and 36% for 24a; (g) acetonitrile, 3 or 4, KI , K_2CO_3 , 90 °C, 41% for 22a and 51% for 25a; (h) 11–16, Et_3N , anhydrous DMF, rt, 4 h, 38–48% for 27a–29a, 74–83% for 30a–32a.

develop a ${}^{99\text{m}}\text{Tc}$ -labeled radioligand as a selective σ_2 receptor probe for tumor imaging with SPECT. The design concept is shown in Figure 1. In the first approach, we directly incorporate the $[(\text{Cp-R})\text{M}(\text{CO})_3]$ ($\text{M} = \text{Re}$, ${}^{99\text{m}}\text{Tc}$) unit containing the carbonyl group in compound 1 with the σ_2 preferring group (5,6-dimethoxyisoindoline moiety in compound 2 or 6,7-dimethoxy-1,2,3,4-tetrahydroisoquinoline moiety in ISO-1) via different carbon chain lengths. In the second approach, the amide group was connected to the $[(\text{Cp-R})\text{M}(\text{CO})_3]$ ($\text{M} = \text{Re}$, ${}^{99\text{m}}\text{Tc}$) unit in compound 1 first and then incorporated with a σ_2 preferring group. Both carbonyl and amide groups are electron-withdrawing groups and would allow the double ligand transfer (DLT) reaction for the efficient synthesis of the ${}^{99\text{m}}\text{Tc}$ -complex from the corresponding ferrocene precursor. In addition, different carbon chain lengths were used as the linker between the $[(\text{Cp-R})\text{M}(\text{CO})_3]$ unit with an electron-withdrawing group and the 5,6-dimethoxyisoindoline or 6,7-dimethoxy-1,2,3,4-tetrahydroisoquinoline pharmacophore to find the optimal

radiotracer with appropriate interaction on σ_2 receptors for *in vivo* tumor imaging. Herein, we report the syntheses of novel $[(\text{Cp-R})\text{M}(\text{CO})_3]$ ($\text{M} = \text{Re}$, ${}^{99\text{m}}\text{Tc}$) complexes containing a 5,6-dimethoxyisoindoline or 6,7-dimethoxy-1,2,3,4-tetrahydroisoquinoline motif, and we evaluated them as potential σ_2 receptor radioligands for tumor imaging *in vivo*.

RESULTS

Chemistry. For the characterization of ${}^{99\text{m}}\text{Tc}$ -labeled compounds, the surrogates of the corresponding rhenium complexes were prepared, and the synthetic routes are depicted in Scheme 1. Intermediates 3,²⁶ 8–10,²⁷ 14–16,²⁷ 17–19,²² and 26²⁸ were obtained according to the methods reported in the literature. *N*-Alkylation of compound 3 or 4 with compounds 17–19 gave compounds 20a–25a (20a, 22a, 23a, and 25a),²⁹ respectively, with yields of 10–51%. It needs to be mentioned that compounds 22a and 25a could be obtained with higher yields in acetonitrile with K_2CO_3 as base than in toluene with

triethylamine. However, N-alkylation of compound 3 with bromine-substituted nitrile, followed by reduction with LiAlH_4 provided compounds 11–13, respectively, with yields of 36–50%. The activated ester 26 reacted with the corresponding amine analogues 11–16 in anhydrous DMF at room temperature to afford the target rhenium analogues 27a–32a (27a, 28a, and 29a).³⁰ Complex 31a could be recrystallized by slow evaporation of a mixture of methylene dichloride and hexane solution to afford X-ray diffraction crystals.

To further confirm the chemical structure and examine the binding model of $^{99\text{m}}\text{Tc}$ -labeled cyclopentadienyl tricarbonyl complexes, the single X-ray crystal structure analysis of complex 31a was performed. Crystal structure data together with details of the determinations are summarized in Tables S1–5. The crystal structure with the atomic numbering scheme of compound 31a is shown in Figure 2. The central rhenium atom is η^5 -coordinated

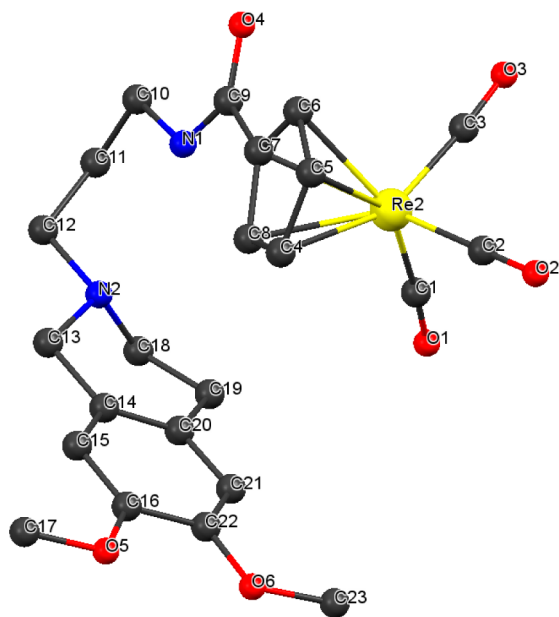


Figure 2. Crystal structure of compound 31a.

to the cyclopentadienyl ring, and the coordination sphere is completed by three carbonyl groups. The average bond lengths of $\text{Re}-\text{C}(\text{Cp})$ and $\text{Re}-\text{C}(\text{CO})$ are 2.30 and 1.91 Å, respectively. The bond angle of $\text{C}-\text{Re}-\text{C}$ (between CO) is approximately 90° . The distance between the N atom and the center of the aromatic ring of 6,7-dimethoxy-1,2,3,4-tetrahydroisoquinoline residue is 3.70 Å. The distance between the N atom and the center of the Cp ring of the $[\text{CpM}(\text{CO})_3]$ core is 5.05 Å.

In Vitro Radioligand Competition Studies. The radioligand competition experiments were conducted as previously reported.²⁰ Typically, (+)-[^3H]pentazocine was used for the σ_1 receptors, and [^3H]1,3-di-*o*-tolyl-guanidine ([^3H]DTG) in the presence of 10 μM dextransorphan was used for the σ_2 receptors. The affinities of the rhenium complexes and ferrocene precursors for σ_1 and σ_2 receptors are listed in Table 1. In general, the carbon length of the linker displayed significant influence on the affinity and subtype selectivity. Rhenium complexes with a carbonyl group displayed higher affinities for σ_2 receptors than those with an amide group (20a–25a vs 27a–32a). Compound 20a and 24a possessed nanomolar affinity for σ_2 receptors and moderate subtype selectivity. Compounds 23a,²⁹ 29a,³⁰ and 30a displayed comparable affinity for σ_2 receptors and subtype selectivity to

Table 1. Binding Affinities of Cyclopentadienyl Tricarbonyl Rhenium Complexes and Ferrocene Precursors for σ_1 and σ_2 Receptors^a

compd	$K_i(\sigma_1)$ (nM)	$K_i(\sigma_2)$ (nM)	$K_i(\sigma_1)/K_i(\sigma_2)$
20a	30.1 ± 11.3	2.96 ± 0.15	10.2
21a	6.67 ± 0.36	17.4 ± 2.2	0.4
22a	5.99 ± 1.72	10.2 ± 4.2	0.6
23a	121 ± 10	20.9 ± 0.2	5.8
24a	19.5 ± 4.2	7.42 ± 1.11	2.6
25a	6.46 ± 1.45	13.9 ± 7.5	0.5
27a	167 ± 49	508 ± 132	0.3
28a	524 ± 6	444 ± 242	1.2
29a	296 ± 104	22.6 ± 0.5	13.1
30a	309 ± 21	35.0 ± 10.1	8.8
31a	146 ± 65	41.0 ± 10.5	3.6
32a	187 ± 3	127 ± 48	1.5
36	137 ± 20	10.5 ± 0.7	13.0
38	19.2 ± 1.6	18.2 ± 3.3	1.1
39	240 ± 115	18.0 ± 1.4	13.3
41	13.3 ± 6.3	10.0 ± 0.3	1.3
43	98 ± 39	15.2 ± 0.1	6.5
44	1300 ± 305	60.2 ± 1.9	21.6
45	181 ± 25	30.0 ± 0.4	6.0
46	155 ± 27	23.5 ± 5.8	6.6
ISO-1 ^b	330 ± 25	6.95 ± 1.63	47.5
ISO-1 ^c	102 ± 15	28.2 ± 0.9	3.6
siramesine ^c	4.69 ± 2.36	3.08 ± 0.68	1.5
siramesine ^d	17	0.12	140
siramesine ^e	10.5 ± 2.6	12.6 ± 0.1	0.8
haloperidol ^f	4.95 ± 1.74	20.7 ± 0.07	0.2

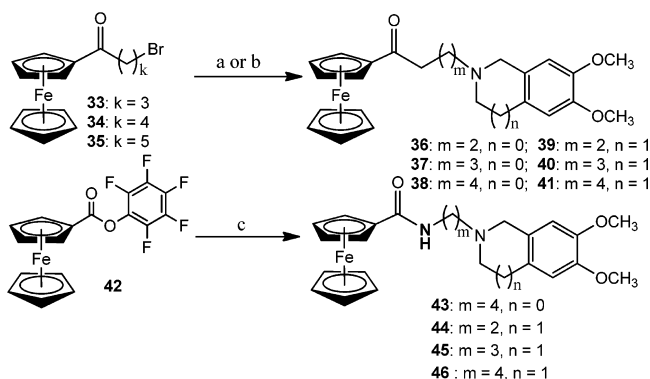
^aValues are the means \pm standard deviation (SD) of at least two experiments performed in triplicate. ^bFrom ref 10. ^cFrom ref 23. ^d IC_{50} value, from ref 31. ^eFrom ref 32. ^fFrom ref 33.

ISO-1. Similar to our previous findings, ferrocene precursors with a carbonyl group displayed comparable affinity for σ_2 receptors to the corresponding rhenium complexes (36 vs 20a, 38 vs 22a, 39 vs 23a, and 41 vs 25a) and a little higher subtype selectivity.

Considering the low nanomolar affinity and subtype selectivity of compound 20a for σ_2 receptors, its affinities for the additional receptors and transporters were further tested. Compound 20a exhibited very low affinity for VACHT ($K_i(\text{VACHT}) = 7026 \pm 163$ nM) and was thus characterized by an excellent selectivity for σ_2 receptors ($K_i(\text{VACHT})/K_i(\sigma_2) = 2374$). Moreover, this ligand also displayed low affinity for dopamine $\text{D}_{2\text{L}}$ receptors, NMDA receptors, opiate receptors, dopamine transporter (DAT), norepinephrine transporter (NET), and serotonin transporter (SERT) as shown in Table S6.

Radiolabeling. Considering the moderate to high affinity and selectivity of the rhenium complexes 20a–25a and 29a–30a for σ_2 receptors, the corresponding $^{99\text{m}}\text{Tc}$ -labeled radiotracers were prepared. The synthetic routes of the ferrocene precursors were similar to those of the corresponding rhenium compounds as shown in Scheme 2. The desired $^{99\text{m}}\text{Tc}$ -labeled radiotracers were obtained via DLT reaction as shown in Scheme 3. After purification by semipreparative high performance liquid chromatography (HPLC), [$^{99\text{m}}\text{Tc}$]20b–25b ([$^{99\text{m}}\text{Tc}$]20b, [$^{99\text{m}}\text{Tc}$]22b, [$^{99\text{m}}\text{Tc}$]23b and [$^{99\text{m}}\text{Tc}$]25b),²⁹ and [$^{99\text{m}}\text{Tc}$]29b–30b ([$^{99\text{m}}\text{Tc}$]29b)³⁰ were obtained with radiochemical yields of 13–67% and a radiochemical purity of >99%.

In Vitro Evaluation of the $^{99\text{m}}\text{Tc}$ -labeled Complexes. **Lipophilicity.** For *in vitro* properties, the lipophilicity of the

Scheme 2. Synthetic Routes for the Ferrocene Precursors^a

^aReagents and conditions: (a) toluene, 3 or 4, KI, Et₃N, 115 °C, 16% for 36, 19% for 37, 33% for 39 and 22% for 40; (b) acetonitrile, 3 or 4, KI, K₂CO₃, 90 °C, 44% for 38 and 78% for 41; (c) 13–16, Et₃N, anhydrous DMF, rt, 4 h, 65% for 43, 69% for 44, 63% for 45, 68% for 46.

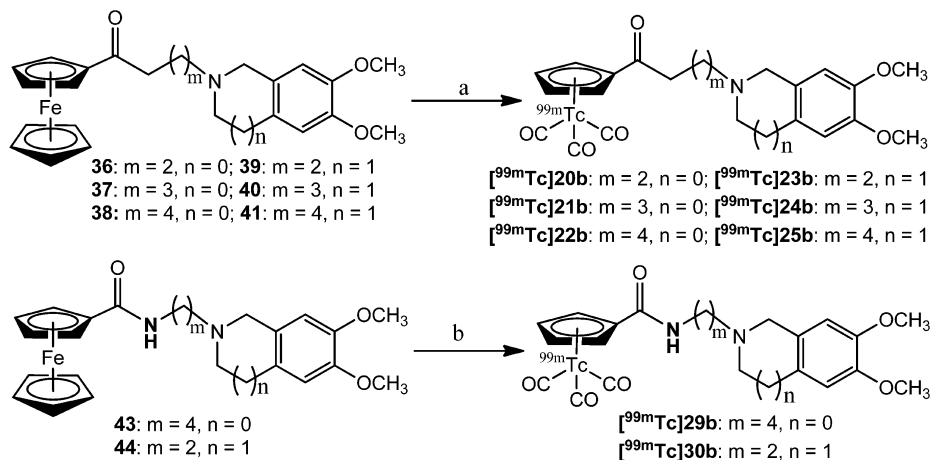
radiotracer is an important factor in the prediction of its free fraction in the plasma, the ability to cross the blood–brain barrier (BBB) and nonspecific binding *in vivo*.^{34,35} The measurement of the partition coefficients between 1-octanol and 0.05 M sodium phosphate buffer at pH 7.4 was executed using a shake flask method.^{22,36} The log *D* values of [^{99m}Tc]20b–25b and [^{99m}Tc]29b–30b were 2.56 ± 0.08,²⁹ 2.44 ± 0.02, 2.56 ± 0.08,²⁹ 2.61 ± 0.05, 2.92 ± 0.02, 2.60 ± 0.06, 2.39 ± 0.05,³⁰ and 1.72 ± 0.09, respectively. The moderate lipophilicity of the above radiotracers may lead to decreased nonspecific binding and enhanced specific binding signal *in vivo*.

In Vitro Evaluation of the ^{99m}Tc-Labeled Complexes in DU145 Prostate Cells. It has been reported that DU145 prostate tumor cells exhibit high expression of both σ₁ and σ₂ receptors.⁴ Considering the affinity and subtype selectivity for σ₂ receptors, the binding assays of the radioligands [^{99m}Tc]20b, [^{99m}Tc]23b, and [^{99m}Tc]29b–30b in DU145 prostate tumor cells were performed. The results are summarized in Figure 3. After incubation for 120 min, the cellular association of [^{99m}Tc]20b and [^{99m}Tc]23b were 8.86% and 2.06%, respectively. For the

complexes with an amide group, the cellular association of [^{99m}Tc]29b and [^{99m}Tc]30b reached 4.91% and 6.89% at 45 min and increased slightly afterward to 5.12% and 7.08% at 120 min, respectively. In blocking studies, treatment with haloperidol and ISO-1 significantly decreased the cellular association of [^{99m}Tc]20b and [^{99m}Tc]23b in a dose-dependent manner, indicating the specific binding of [^{99m}Tc]20b and [^{99m}Tc]23b to σ₂ receptors in DU145 cells. Moreover, treatment with various concentrations of haloperidol led to decreased association of [^{99m}Tc]29b and [^{99m}Tc]30b in a dose-dependent manner. However, [^{99m}Tc]29b showed a higher blocking percentage than [^{99m}Tc]30b (66% vs 47%) at the same concentration of haloperidol (10^{−4} M), suggesting a higher specific binding of [^{99m}Tc]29b to σ receptors in DU145 cells.

In Vitro Evaluation of the ^{99m}Tc-Labeled Complexes in C6 Glioma Cells. C6 glioma tumor cells, with high expression of σ₂ receptors and low expression of σ₁ receptors,³ were selected for further evaluation of [^{99m}Tc]20b and [^{99m}Tc]29b. The results are shown in Figure 4. High cellular association of [^{99m}Tc]20b was observed in a time-dependent manner. The association reached 25% after incubation for 120 min. Furthermore, coinubation with different concentrations of ISO-1 led to remarkably decreased association in a dose-dependent manner. The cellular association was significantly reduced by about 80% with 10^{−6} M of ISO-1, suggesting high specific binding of [^{99m}Tc]20b to σ₂ receptors in C6 glioma cells. However, much lower uptake of [^{99m}Tc]29b (<1.49%) was observed. Treatment with different concentrations of haloperidol also led to reduced association of [^{99m}Tc]29b, but the blocking percentage was low (37% with 10^{−4} M of haloperidol). In other words, [^{99m}Tc]20b displayed higher association and higher specific binding to σ₂ receptors than [^{99m}Tc]29b in C6 glioma cells.

Since compounds 21a and 24a had moderate to high affinity for σ₂ receptors, the binding assays of the corresponding [^{99m}Tc]21b and [^{99m}Tc]24b were performed in C6 glioma cells. The results are provided in Figure S3. The cellular association of [^{99m}Tc]21b and [^{99m}Tc]24b was 4.88% and 5.12%, respectively, but treatment with 10^{−6} M of haloperidol only led to minimal reduction of the cellular association, suggesting high nonspecific binding of [^{99m}Tc]21b and [^{99m}Tc]24b in C6 glioma cells.

Scheme 3. Synthesis of the ^{99m}Tc-Labeled Complexes from the Ferrocene Precursors^a

^aReagents and conditions: (a) ^{99m}TcO₄[−], Mn(CO)₅, DMF, 140 °C, 1 h, 13–32% for [^{99m}Tc]20b, 37–59% for [^{99m}Tc]21b, 25–33% for [^{99m}Tc]22b, 34–53% for [^{99m}Tc]23b, 44–62% for [^{99m}Tc]24b, 57–63% for [^{99m}Tc]25b; (b) ^{99m}TcO₄[−], Mn(CO)₅, DMF, 150 °C, 1 h, 36–67% for [^{99m}Tc]29b, 48–60% for [^{99m}Tc]30b.

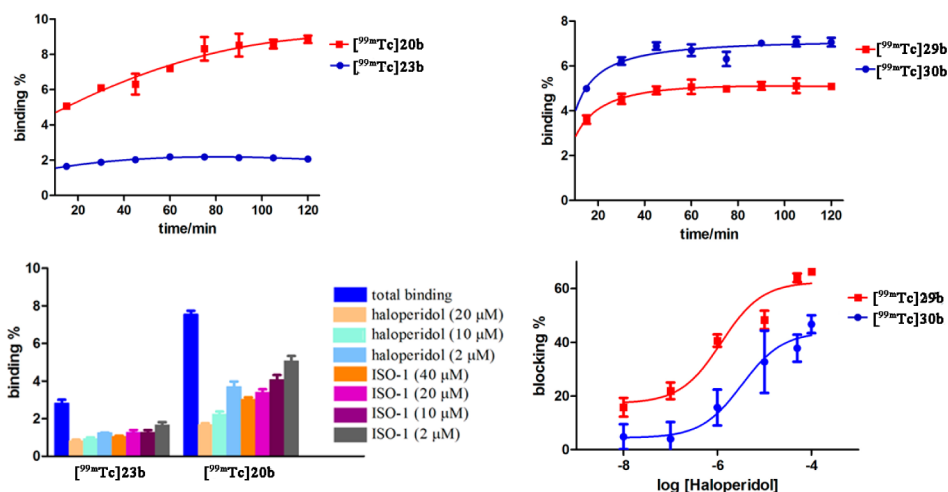


Figure 3. *In vitro* studies on cellular association of [^{99m}Tc]20b, [^{99m}Tc]23b, [^{99m}Tc]29b, and [^{99m}Tc]30b in DU145 prostate tumor cells.

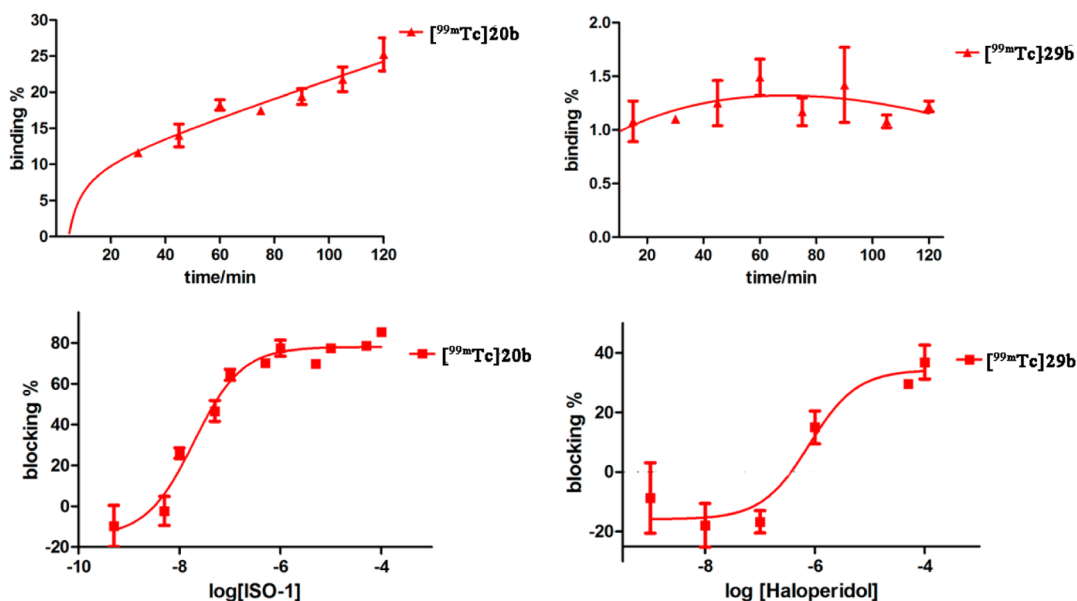


Figure 4. *In vitro* studies on cellular association of [^{99m}Tc]20b and [^{99m}Tc]29b in C6 glioma cells.

Table 2. Biodistribution of [^{99m}Tc]20b in Male ICR Mice^a

organ	2 min	15 min	30 min	60 min	120 min	240 min
blood	1.82 ± 0.18	0.81 ± 0.07	0.71 ± 0.07	0.57 ± 0.11	0.43 ± 0.07	0.31 ± 0.04
brain	2.57 ± 0.31	2.70 ± 0.18	2.08 ± 0.22	1.06 ± 0.17	0.47 ± 0.08	0.17 ± 0.04
heart	11.81 ± 1.58	3.25 ± 0.22	2.07 ± 0.23	1.31 ± 0.21	0.83 ± 0.14	0.43 ± 0.07
liver	4.76 ± 1.29	10.03 ± 0.61	12.51 ± 1.88	13.41 ± 0.71	16.14 ± 1.73	17.33 ± 3.11
spleen	3.43 ± 0.89	7.46 ± 0.81	7.15 ± 1.44	4.67 ± 0.38	2.76 ± 0.58	1.24 ± 0.36
lung	29.38 ± 4.97	9.61 ± 2.58	7.14 ± 2.44	3.77 ± 0.80	2.19 ± 0.69	1.47 ± 0.53
kidney	14.46 ± 1.08	15.48 ± 1.92	11.78 ± 1.04	8.92 ± 1.17	6.62 ± 0.99	6.11 ± 1.21
small intestine ^b	4.07 ± 0.70	11.05 ± 1.77	11.69 ± 3.19	14.01 ± 2.20	15.08 ± 1.87	12.94 ± 2.36
stomach ^b	0.96 ± 0.09	2.42 ± 0.74	2.67 ± 0.74	1.46 ± 0.40	1.56 ± 0.77	1.23 ± 0.26
muscle	2.42 ± 0.78	2.16 ± 0.22	1.74 ± 0.20	1.40 ± 0.18	0.78 ± 0.23	0.24 ± 0.11
thyroid ^b	0.20 ± 0.03	0.17 ± 0.05	0.17 ± 0.03	0.09 ± 0.02	0.12 ± 0.01	0.08 ± 0.03

^aData are expressed as a percentage of injected dose per gram, means ± SD, $n = 5$. ^bPercentage of injected dose per organ.

***In Vivo* Evaluation of the ^{99m}Tc -Labeled Complexes.** **Biodistribution and Blocking Studies in Male ICR Mice.** To investigate the kinetics of the radiotracers, we performed biodistribution and blocking studies of [^{99m}Tc]20b, [^{99m}Tc]23b, [^{99m}Tc]25b, and [^{99m}Tc]29b in ICR mice. The results are

summarized in Tables 2–4, Figure 5, and Table S7 and Figure S4. Both [^{99m}Tc]20b and [^{99m}Tc]23b exhibited high initial brain uptake with $2.57 \pm 0.31\%$ inject dose (ID)/g and $2.38 \pm 0.31\%$ ID/g at 2 min, respectively, and fast washout with $0.17 \pm 0.04\%$ ID/g and $0.09 \pm 0.01\%$ ID/g, respectively, at 240 min. However,

Table 3. Biodistribution of [^{99m}Tc]23b in Male ICR Mice^a

organ	2 min	15 min	30 min	60 min	120 min	240 min
blood	2.11 ± 0.15	1.06 ± 0.09	0.89 ± 0.07	0.74 ± 0.06	0.54 ± 0.11	0.44 ± 0.15
brain	2.38 ± 0.31	1.79 ± 0.20	1.08 ± 0.13	0.52 ± 0.02	0.20 ± 0.02	0.09 ± 0.01
heart	8.73 ± 0.81	1.93 ± 0.13	1.29 ± 0.09	0.79 ± 0.09	0.51 ± 0.02	0.34 ± 0.02
liver	7.51 ± 1.11	13.91 ± 0.92	17.03 ± 1.13	20.36 ± 1.30	22.63 ± 1.38	22.82 ± 3.22
spleen	4.39 ± 1.34	5.59 ± 0.51	4.08 ± 0.48	2.64 ± 0.13	1.20 ± 0.23	0.66 ± 0.22
lung	27.20 ± 5.00	7.13 ± 1.54	4.10 ± 1.23	2.67 ± 0.80	1.76 ± 0.40	1.29 ± 0.23
kidney	18.88 ± 1.30	12.45 ± 1.30	9.91 ± 0.94	10.32 ± 1.37	9.86 ± 1.09	9.22 ± 1.82
small intestine ^b	6.13 ± 1.02	8.75 ± 2.27	11.22 ± 1.74	15.53 ± 2.24	19.15 ± 2.63	15.89 ± 1.14
stomach ^b	1.32 ± 0.29	2.54 ± 0.44	2.74 ± 0.24	3.27 ± 0.13	2.77 ± 0.45	1.58 ± 0.57
muscle	2.67 ± 0.35	1.66 ± 0.23	1.22 ± 0.15	0.75 ± 0.11	0.38 ± 0.06	0.21 ± 0.07
thyroid ^b	0.11 ± 0.05	0.18 ± 0.05	0.08 ± 0.01	0.11 ± 0.01	0.09 ± 0.04	0.07 ± 0.02

^aData are expressed as the percentage of injected dose per gram, means ± SD, *n* = 5. ^bPercentage of injected dose per organ.

Table 4. Biodistribution of [^{99m}Tc]29b in Male ICR Mice^a

organ	2 min	15 min	30 min	60 min	120 min	240 min
blood	2.04 ± 0.29	0.74 ± 0.06	0.53 ± 0.03	0.43 ± 0.05	0.41 ± 0.04	0.34 ± 0.03
brain	0.24 ± 0.06	0.21 ± 0.02	0.16 ± 0.02	0.11 ± 0.02	0.11 ± 0.01	0.10 ± 0.01
heart	11.22 ± 1.20	3.27 ± 0.20	2.27 ± 0.24	1.74 ± 0.13	1.45 ± 0.20	1.01 ± 0.16
liver	9.27 ± 1.69	18.56 ± 2.62	24.43 ± 1.60	27.13 ± 2.13	27.98 ± 2.32	28.45 ± 3.32
spleen	5.08 ± 1.42	7.32 ± 0.65	4.50 ± 0.64	1.91 ± 0.58	1.21 ± 0.18	0.78 ± 0.12
lung	31.54 ± 3.28	12.11 ± 2.08	8.93 ± 1.88	7.63 ± 2.40	4.17 ± 0.42	4.03 ± 0.54
kidney	27.45 ± 4.91	17.68 ± 3.19	14.62 ± 0.61	12.14 ± 1.81	10.21 ± 0.51	8.79 ± 1.04
small intestine ^b	6.00 ± 1.31	13.15 ± 1.09	10.62 ± 2.49	11.92 ± 3.25	22.56 ± 3.75	17.64 ± 4.15
stomach ^b	1.27 ± 0.32	2.59 ± 0.47	2.58 ± 1.16	2.17 ± 0.79	2.32 ± 0.92	1.46 ± 0.41
muscle	4.12 ± 0.61	2.02 ± 0.16	1.44 ± 0.21	0.98 ± 0.13	0.68 ± 0.10	0.41 ± 0.03
thyroid ^b	0.11 ± 0.02	0.08 ± 0.02	0.14 ± 0.03	0.09 ± 0.01	0.06 ± 0.01	0.05 ± 0.03

^aData are expressed as the percentage of injected dose per gram, means ± SD, *n* = 5. ^bPercentage of injected dose per organ.

[^{99m}Tc]25b exhibited lower brain uptake (1.05 ± 0.06% ID/g) and relatively slow washout with 0.32 ± 0.04% ID/g at 240 min. [^{99m}Tc]20b, [^{99m}Tc]23b, and [^{99m}Tc]25b exhibited fast clearance from blood and muscle. Low accumulation in the blood of the above radiotracers was observed with 0.31 ± 0.04% ID/g, 0.44 ± 0.15% ID/g, and 0.30 ± 0.05% ID/g at 240 min, respectively. Low accumulation in the muscle was also observed with 0.24 ± 0.11% ID/g, 0.21 ± 0.07% ID/g, and 0.49 ± 0.05% ID/g at 240 min, respectively. In biodistribution studies of [^{99m}Tc]29b (Table 4), much lower brain uptake was observed with 0.24 ± 0.06% ID/g at 2 min, indicating that the amide group had a negative effect on the potential of the radiotracer to cross the BBB. Low accumulation of this radiotracer in blood and muscle at 240 min was observed.

To examine the specific binding of the radiotracers to σ receptors *in vivo*, blocking studies were carried out by administration of haloperidol (1.0 mg/kg) 5 min prior to the radiotracer administration. Pretreatment with haloperidol significantly reduced the accumulation of [^{99m}Tc]20b, [^{99m}Tc]23b, and [^{99m}Tc]29b in the brain by 43%, 45%, and 36%, respectively, at 120 min after injection (Figure 5). Moreover, remarkable reduction of radiotracers in the organs known to express σ receptors was observed, indicating the specific binding of [^{99m}Tc]20b, [^{99m}Tc]23b, and [^{99m}Tc]29b to σ receptors *in vivo*. However, there is no significant reduction of radiotracer accumulation observed in the brain for [^{99m}Tc]25b (Figure S4), suggesting the high nonspecific binding of [^{99m}Tc]25b *in vivo*.

Biodistribution and Blocking Studies of [^{99m}Tc]20b in Balb/c Nude Mice Bearing C6 Glioma Xenografts. Encouraged by the optimal properties of [^{99m}Tc]20b *in vitro* and *in vivo*, biodistribution and blocking studies of this

radiotracer were performed in Balb/c nude mice bearing C6 glioma xenografts. The results are shown in Table 5 and Figure 6. High accumulation of the radiotracer in the tumor was observed with 5.41 ± 0.91% ID/g at 120 min and 5.92 ± 1.30% ID/g at 240 min. At the same time, low accumulation of the radiotracer in blood and muscle were observed as well. Therefore, high tumor/blood ratios and tumor/muscle ratios were obtained with 20.6 and 16.1 at 240 min, respectively. To further examine the specific binding to σ receptors in the tumor, blocking studies with haloperidol, ferrocene precursor 36, and siramesine as blocking agents were performed. Pretreatment of haloperidol, 36, and siramesine led to significant reduction of tumor accumulation by 33%, 62%, and 44% at 240 min, respectively, indicating the specific binding of [^{99m}Tc]20b to σ receptors in the tumor. In addition, a reduction of radiotracer in the organs known to contain σ receptors such as the brain, heart, and lung were observed, which is consistent with the biodistribution results in normal mice.

Small Animal SPECT/CT Imaging of [^{99m}Tc]20b. To further confirm the potential applications of [^{99m}Tc]20b in tumor imaging, small animal SPECT/CT scans of the C6 glioma xenograft mouse model were performed using NanoScan SPECT/CT. Representative transverse plane SPECT/CT images at 180 min after injection of [^{99m}Tc]20b (22.2 MBq, 0.15 mL) are shown in Figure 7, and the coronal and sagittal plane images are shown in the Figure S5. The solid tumor was clearly visualized with high tumor-to-background contrast, indicating that [^{99m}Tc]20b could determine the level of σ_2 receptors in solid tumors *in vivo*.

In Vivo Radiometabolic Stability of [^{99m}Tc]20b. The metabolic stability of [^{99m}Tc]20b was investigated in brain and

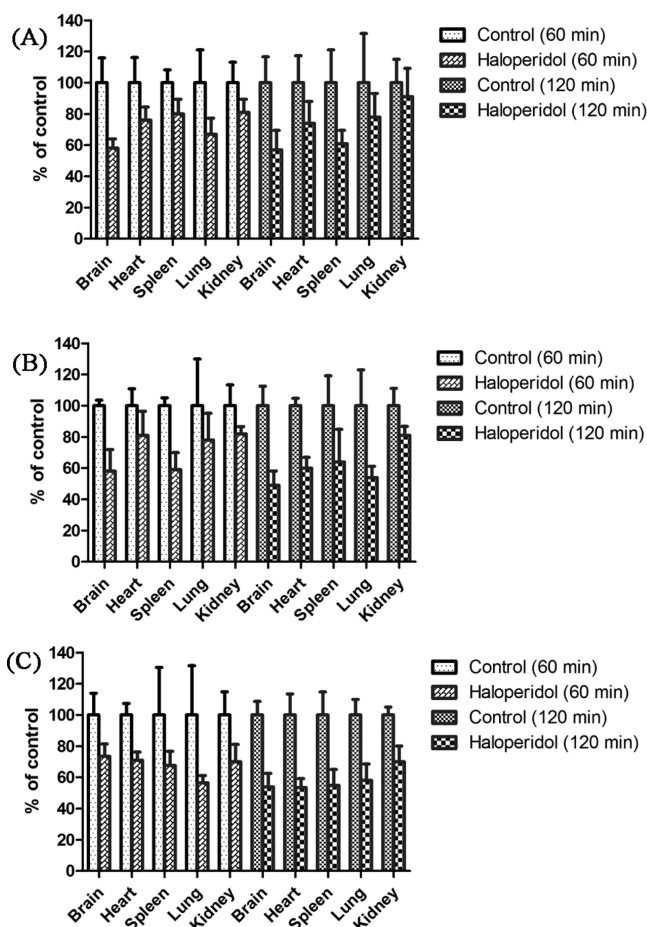


Figure 5. Effects of pretreatment with haloperidol (0.1 mL, 1.0 mg/kg) on organ biodistribution of [^{99m}Tc]20b (A), [^{99m}Tc]23b (B), or [^{99m}Tc]29b (C) in male ICR mice ($n = 5$). Student's t test (independent, two-tailed) was performed, and $p < 0.05$ (except for [^{99m}Tc]20b in the lungs and kidney at 120 min after intravenous injection, [^{99m}Tc]23b in the heart and lungs at 60 min after intravenous injection, and [^{99m}Tc]29b in the spleen at 60 min after intravenous injection).

Table 5. Biodistribution of [^{99m}Tc]20b in Balb/c Nude Mice Bearing C6 Glioma Xenografts^a

organ	120 min	240 min
blood	0.32 ± 0.05	0.28 ± 0.03
brain	0.68 ± 0.21	0.30 ± 0.05
heart	0.80 ± 0.09	0.55 ± 0.08
liver	18.44 ± 3.58	22.47 ± 2.37
spleen	5.48 ± 0.58	2.69 ± 0.20
lung	2.92 ± 0.74	2.04 ± 0.49
kidney	6.86 ± 1.16	5.93 ± 0.62
small intestine ^b	15.26 ± 1.06	16.33 ± 3.12
stomach ^b	0.82 ± 0.19	0.83 ± 0.34
muscle	0.65 ± 0.11	0.37 ± 0.06
thyroid ^b	0.08 ± 0.01	0.08 ± 0.01
tumor	5.41 ± 0.91	5.92 ± 1.30
tumor/blood	17.5 ± 4.0	20.6 ± 4.1
tumor/muscle	8.5 ± 1.6	16.1 ± 5.3

^aData are expressed as the percentage of injected dose per gram, means ± SD, $n = 5$. ^bPercentage of injected dose per organ.

liver samples of ICR mice 15 and 30 min after the injection of the radiotracer. The HPLC chromatograms are shown in Figure 8.

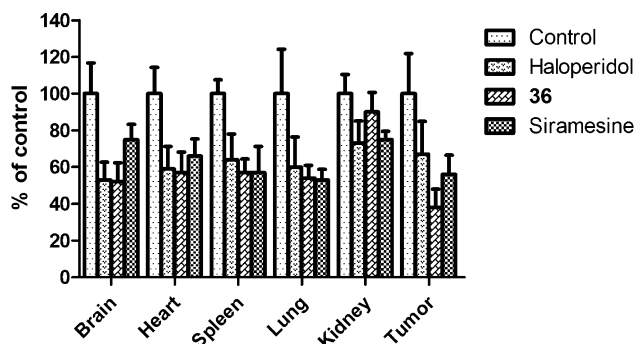


Figure 6. Effects of pretreatment with haloperidol, 36, and siramesine (0.1 mL, 1.0 mg/kg) on organ biodistribution of [^{99m}Tc]20b in Balb/c nude mice bearing C6 glioma xenografts. Student's t test (independent, two-tailed) was performed, and $p < 0.05$ (except in the kidney with 36 and in the tumor with haloperidol at 240 min after intravenous injection).

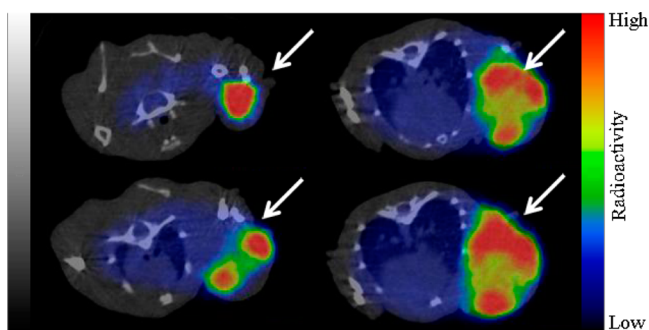


Figure 7. Representative transverse plane slices of NanoScan SPECT/CT fusion images of [^{99m}Tc]20b (22.2 MBq, 0.15 mL) in male Balb/c nude mouse bearing C6 glioma xenografts at 180 min after injection. Isoflurane was used for anesthesia.

The parent radiotracer [^{99m}Tc]20b was the main radioactive compound presented in the brain at both 15 and 30 min, indicating that [^{99m}Tc]20b was very stable in the brain and that there was no entry of radioactive metabolites into the brain. In the liver samples, three main metabolites with retention times of 2.4 min (M1), 4.6 min (M2), and 5.4 min (M3), respectively, were observed. Furthermore, the percentage of the parent compound [^{99m}Tc]20b was decreased with time (31.8% and 16.1% at 15 and 30 min, respectively). The percentage of M1 was significantly increased with 45.8% and 65.6% at 15 and 30 min, respectively.

DISCUSSION

A number of studies have demonstrated the high expression of σ_2 receptors in many human tumors.^{2–4} The σ_2 receptor has proved to be a unique biomarker of proliferative status in solid tumors.^{7–9} Therefore, the development of molecular probes for imaging σ_2 receptors will provide useful information on the proliferative status of tumors in patients. Recently, [^{18}F]ISO-1 was developed as a potential σ_2 receptor PET radiotracer for imaging the proliferative status of tumors.^{10–12} However, there is still need for a σ_2 receptor SPECT imaging radioligands in clinical trials. ^{99m}Tc is the most common and convenient nuclide for SPECT imaging in clinical use. Furthermore, $^{99m}\text{Tc}/^{188}\text{Re}$ is considered as the ideal “matched pair” of theragnostic radio-nuclides. Development of the ^{99m}Tc -labeled radiotracer will provide useful information on the synthesis and therapeutic

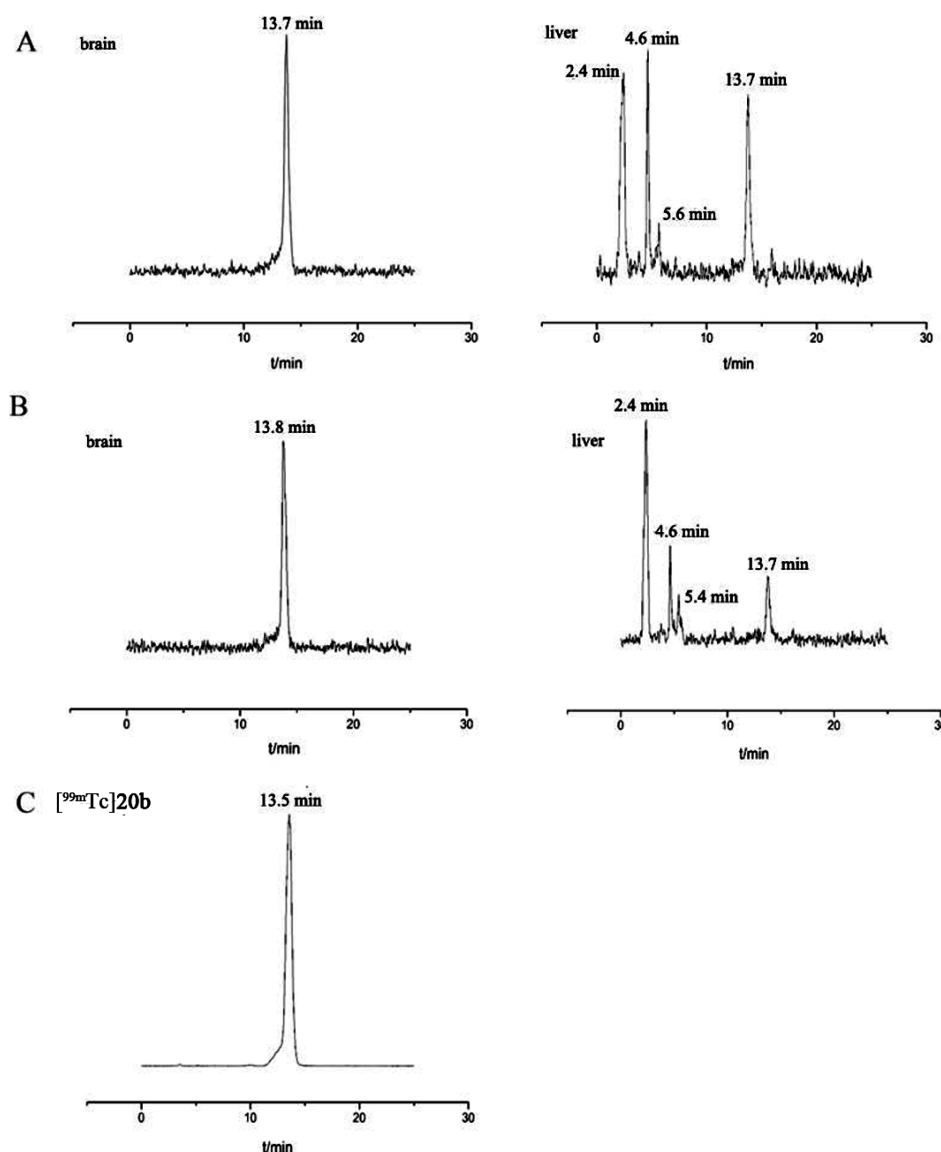


Figure 8. Analytical HPLC chromatograms of radioactive compounds in mouse brain and liver samples after intravenous injection of $[^{99m}\text{Tc}]20b$ (18.5 MBq, 0.15 mL). (A) Brain and liver samples at 15 min. (B) Brain and liver samples at 30 min. (C) $[^{99m}\text{Tc}]20b$.

doses of the corresponding ^{188}Re -labeled radiopharmaceuticals. Therefore, ^{99m}Tc -labeled radiotracers for σ_2 receptors imaging not only could be used in the early diagnosis of cancer but also could provide useful information for the therapeutic tumor medicine of ^{188}Re -labeled radiopharmaceuticals. $[^{99m}\text{Tc}]$ $[N$ -[2-((3'- N' -propyl-[3,3,1]aza-bicyclononan-3 α -yl)(2''-methoxy-5-methyl-phenylcarbamate)(2-mercapttoethyl)amino)acetyl]-2-amino-ethanethiolato]technetium(V) oxide ($[^{99m}\text{Tc}]47$) was the most potential σ_2 receptor radiotracer ever reported with moderate affinity for σ_2 receptors ($K_i = 22$ nM) and high subtype selectivity as well as visualization of tumor shape in planar gamma imaging.¹⁸ However, no further evaluation, such as SPECT/CT imaging, was reported since 2001. To the best of our knowledge, only the radiotracers with high tumor uptakes and high tumor-to-muscle ratios could have potential applications in the early diagnosis of tumor. Because of the much higher expression of the σ_2 receptors in tumors and moderate to high expression of the σ_1 receptors in the normal organs, development of highly subtype selective ^{99m}Tc -labeled σ_2 receptor radioligands with high tumor uptakes and high tumor/background ratios will have wide

applications in imaging the proliferative status in solid tumors. Our aim in this article is to develop novel ^{99m}Tc -labeled radiotracers with high affinity for σ_2 receptors and high selectivity as well as clear visualization of solid tumors.

Enlightened by our previous results of ^{99m}Tc -labeled radiotracers with the $[(\text{Cp-R})\text{Tc}(\text{CO})_3]$ unit,^{22,25} we replaced the aromatic ring of ISO-1 with a $[(\text{Cp-R})\text{M}(\text{CO})_3]$ unit with an electron-withdrawing group and connected it to a 5,6-dimethoxyisindoline or 6,7-dimethoxy-1,2,3,4-tetrahydroisquinoline scaffold via different carbon length linkers. The designed complexes were in accordance with the σ_2 receptor ligand pharmacophore model proposed by Glennon with an amine binding site flanked by two hydrophobic regions.³⁷ It is encouraging that complexes **20a**, **23a**, **29a**, and **30a** have high affinity and subtype selectivity for σ_2 receptors. Among these ligands, compound **20a** had low nanomolar affinity and higher subtype selectivity than ISO-1. Moreover, it showed high selectivity toward VACHT (2374-fold), dopamine D_{2L} receptors, NMDA receptors, opiate receptors, DAT, NET, and SERT.

To detect the specific binding of the radiotracers to σ_2 receptors, we selected DU145 human prostate tumor cells (B_{\max} values of σ_1 and σ_2 receptors were 1800 and 1930 fmol/mg protein, respectively)⁴ and C6 rat glioma cells (B_{\max} values of σ_1 and σ_2 receptors were 42 and 5507 fmol/mg protein, respectively).⁵ In the *in vitro* binding assays in tumor cells, [^{99m}Tc]20b exhibited much higher cellular association and comparable specific binding to σ_2 receptors in DU145 cells than [^{99m}Tc]23b, which is in good agreement with the higher affinity of the former compound. Coincubation with ISO-1 led to significant reduction of cellular association in a dose-dependent manner, indicating the specific binding of [^{99m}Tc]20b to σ_2 receptors. [^{99m}Tc]29b exhibited comparable cellular association and higher specific binding to σ receptors in DU145 cells than [^{99m}Tc]30b. Thus, it seemed that the 5,6-dimethoxyisoindoline moiety is a better σ_2 preferring group than the 6,7-dimethoxy-1,2,3,4-tetrahydroisoquinoline moiety. In C6 glioma cells, [^{99m}Tc]20b displayed much higher cellular association and higher specific binding to σ receptors than [^{99m}Tc]29b, indicating that [^{99m}Tc]20b is the most potent radioligand in this series and warrants further evaluation.

To investigate the kinetics and examine the specific binding of the radiotracers *in vivo*, biodistribution studies of [^{99m}Tc]20b, [^{99m}Tc]23b, and [^{99m}Tc]29b were performed in male ICR mice. [^{99m}Tc]20b and [^{99m}Tc]23b displayed high initial brain uptake with 2.57 and 2.38% ID/g at 2 min after injection, respectively. [^{99m}Tc]29b exhibited low brain uptake with 0.24% ID/g at 2 min after injection, indicating that the amide and carbonyl group showed different influences on the potential of the radiotracer to cross the BBB. Interestingly, all the radiotracers mentioned above exhibited fast clearance from the muscle and blood, which is very important for tumor imaging agents. Pretreatment with haloperidol significantly reduced the accumulation in the brain, indicating the specific binding of [^{99m}Tc]20b, [^{99m}Tc]23b, and [^{99m}Tc]29b to σ receptors *in vivo*.

Finally, we selected the most potent radioligand [^{99m}Tc]20b and evaluated its potential applications in tumor imaging. In biodistribution studies in Balb/c nude mice bearing C6 glioma xenografts, [^{99m}Tc]20b showed much higher tumor uptake (5.41–5.92% ID/g) than [^{99m}Tc]47 (1.11–2.11% ID/g, 66 murine breast tumor)¹⁸ and [¹⁸F]ISO-1 (0.64–3.67% ID/g, EMT-6 mouse mammary tumor).¹⁰ [^{99m}Tc]20b also exhibited fast clearance from the surrounding tissues. Thus, the tumor-to-muscle ratios (8.5–16.1) are higher than those of [^{99m}Tc]47 (0.57–4.95) (16 vs 4.95 at 4 h).¹⁸ Moreover, the tumor-to-blood ratios (17.5–20.6) are significantly higher than those of [^{99m}Tc]47 (0.56–2.21)¹⁸ and [¹⁸F]ISO-1 (1.47–2.19).¹⁰ Pretreatment with haloperidol, 36, and siramesine resulted in a remarkable reduction of radiotracer accumulation in the tumors, indicating the specific binding of [^{99m}Tc]20b to σ receptors in C6 glioma tumors *in vivo*. Consistent with the high tumor uptakes and high tumor-to-muscle ratios in biodistribution studies, the animal SPECT/CT imaging of [^{99m}Tc]20b demonstrated a high uptake and clear visualization of C6 glioma xenografts in nude mice at 180 min. These data suggest the potential use of [^{99m}Tc]20b for SPECT imaging studies of brain tumors in patients.

CONCLUSIONS

By applying an integrated strategy, we have designed, prepared, and evaluated a series of cyclopentadienyl tricarbonyl ^{99m}Tc/Re complexes containing 5,6-dimethoxyisoindoline or 6,7-dimethoxy-1,2,3,4-tetrahydroisoquinoline moiety. Compared with ISO-1, the rhenium complex of the corresponding radiotracer

20a possessed higher affinity and subtype selectivity for σ_2 receptors. The corresponding radiotracer [^{99m}Tc]20b showed high uptakes and specific binding to σ receptors in DU145 prostate cells and C6 glioma cells. Moreover, [^{99m}Tc]20b exhibited high tumor uptake and high tumor/blood and tumor/muscle ratios in nude mice bearing C6 glioma xenografts. Furthermore, this radiotracer demonstrated specific binding to σ receptors in the tumor. In particular, animal SPECT/CT imaging studies with [^{99m}Tc]20b demonstrated a high uptake and clear visualization of C6 glioma xenografts in nude mice. These findings demonstrated that the further evaluation of [^{99m}Tc]20b as a potential σ_2 receptor probe for imaging the proliferative status in brain tumors is worth doing.

EXPERIMENTAL SECTION

All reagents used in the synthesis were commercial products and were used without further purification unless otherwise indicated. ^{99m}Tc-pertechnetate was eluted from a commercial ⁹⁹Mo–^{99m}Tc generator obtained from Beijing Atomic High-tech Co. The ¹H NMR spectra were recorded on Bruker Avance III NMR (400 MHz) spectrometers in CDCl₃ solutions at room temperature with TMS as an internal standard. Chemical shifts (δ) were reported in ppm values relative to the internal TMS. Coupling constants (*J*) were reported in Hertz (Hz). Multiplicity is defined by s (singlet), d (doublet), t (triplet), and m (multiplet). The ¹³C NMR spectra were recorded on Bruker Avance III NMR (100 MHz) spectrometers. Mass spectra were acquired by Quattro micro API ESI/MS (Waters, USA). High-resolution mass spectrometry (HRMS) was performed on a LCT Premier XE ESI-TOF mass spectrometry instrument (Waters, USA). X-ray crystallography data were collected on a Bruker Smart APEX II diffractometer (Bruker Co., Germany). The melting point (Mp) of solid compounds was tested on a WRX-4 micro melting point apparatus (Shanghai yice instrument Co., LTD, China) and was uncorrected. Reactions were monitored by TLC (TLC Silica gel 60 F254, Merck). Flash column chromatography was conducted using silica gel (45–75 μ m) from Qingdao Haiyang Chemical Co., Ltd. The compounds were visualized by illumination with a short wavelength UV lamp (λ = 254 nm). High performance liquid chromatography (HPLC) separations and analyses were performed on a Waters 600 system (Waters, corporation, USA) equipped with a Waters 2489 UV–VIS detector and a Raytest Gabi NaI (Tl) scintillation detector (Raytest, Germany) and on a Shimadzu SCL-20AVP system (Shimadzu Corporation, Japan) equipped with a Bioscan Flow Count 3200 NaI/PMT γ -radiation scintillation detector. Samples were analyzed and separated on an Agela Venusil MP C18 column (250 mm \times 4.6 mm, 5 μ m) using acetonitrile with 0.1% trifluoroacetic acid (TFA) and water with 0.1% TFA as the mobile phase at a flow rate of 1 mL/min. All of the final compounds were analyzed by HPLC with a purity of more than 95% (HPLC profiles are shown in the Supporting Information).

Male ICR mice (4–5 weeks, 22–25 g) were purchased from Vital River Laboratory Animal Technology Co. Ltd. All procedures related to animal experiments were performed in compliance with relevant laws and institutional guidelines. All protocols requiring the use of mice were approved by the animal care committee of Beijing Normal University.

Chemistry. 2-(5,6-Dimethoxyisoindolin-2-yl)acetonitrile (5). Compound 3 (254.0 mg, 1.42 mmol) and 5 mL of triethylamine were dissolved in 10 mL of CH₂Cl₂, followed by the addition of 2-bromoacetonitrile (200.0 mg, 1.67 mmol). The reaction mixture was stirred at room temperature for 24 h. The mixture was then washed with H₂O and extracted with CH₂Cl₂. The organic layer was dried over MgSO₄, filtered, and concentrated under vacuum. The residue was purified by silica gel chromatography (dichloromethane/methanol = 100:1) to afford 5 (219.4 mg, 72%) as a white solid. Mp: 125.5–125.9 °C. ¹H NMR (400 MHz, CDCl₃) δ 6.76 (s, 2H), 4.07 (s, 4H), 3.87 (s, 6H), 3.81 (s, 2H). ESI-MS: [*M* + H]⁺ (*m/z* = 219.2).

3-(5,6-Dimethoxyisoindolin-2-yl)propanenitrile (6). The procedure described for the synthesis of 5 was applied to compound 3 (251.2 mg, 1.40 mmol) and 3-bromopropanenitrile (223.7 mg, 1.67 mmol) to afford 6 (215.5 mg, 67%) as a light brown solid. Mp: 137.1–137.5 °C.

¹H NMR (400 MHz, CDCl₃) δ 6.75 (s, 2H), 4.03 (s, 4H), 3.86 (s, 6H), 3.12 (t, J = 7.0 Hz, 2H), 2.65 (t, J = 6.4 Hz, 2H). ESI-MS: [M + H]⁺ (m/z = 233.2).

4-(5,6-Dimethoxyisoindolin-2-yl)butanenitrile (7). The procedure described for the synthesis of **5** was applied to **3** (254.5 mg, 1.42 mmol) and 4-bromobutanenitrile (247.2 mg, 1.67 mmol) to afford **7** (254.9 mg, 73%) as a light brown solid. ¹H NMR (400 MHz, CDCl₃) δ 6.75 (s, 2H), 4.04 (s, 4H), 3.87 (s, 6H), 2.97 (t, J = 6.7 Hz, 2H), 2.55 (t, J = 7.1 Hz, 2H), 2.02 (t, J = 6.7 Hz, 2H). ESI-MS: [M + H]⁺ (m/z = 247.2).

2-(5,6-Dimethoxyisoindolin-2-yl)ethanamine (11). A solution of LiAlH₄ (145.7 mg, 3.83 mmol) in 10 mL of anhydrous diethyl ether was cooled at 0 °C (ice bath), followed by the addition of a solution of **5** (210.0 mg, 0.96 mmol) in 5 mL of anhydrous THF. Then, the reaction mixture was stirred at room temperature overnight. The reaction mixture was quenched with ice–H₂O and extracted with ethyl acetate. The organic layer was dried over anhydrous MgSO₄, filtered, and concentrated under vacuum. The residue was purified by silica gel chromatography (dichloromethane/methanol/triethylamine = 20:1:1) to give **11** (97.2 mg, 46%) as a light yellow oil. ¹H NMR (400 MHz, CDCl₃) δ 6.75 (s, 2H), 3.91 (s, 4H), 3.86 (s, 6H), 2.90–2.87 (m, 2H), 2.84–2.81 (m, 2H), 2.04 (br s, 2H). ESI-MS: [M + H]⁺ (m/z = 223.2).

3-(5,6-Dimethoxyisoindolin-2-yl)propan-1-amine (12). The procedure described for the synthesis of **11** was applied to LiAlH₄ (130.5 mg, 3.44 mmol) and compound **6** (200.0 mg, 0.86 mmol) to afford **12** (73.0 mg, 36%) as a brown oil. ¹H NMR (400 MHz, CDCl₃) δ 6.75 (s, 2H), 4.07 (s, 4H), 3.83 (s, 6H), 3.15 (q, 2H, J = 7.3 Hz), 1.74–1.67 (m, 2H), 1.47–1.32 (m, 2H). ESI-MS: [M + H]⁺ (m/z = 237.2).

4-(5,6-Dimethoxyisoindolin-2-yl)butan-1-amine (13). The procedure described for the synthesis of **11** was applied to LiAlH₄ (129.0 mg, 3.40 mmol) and compound **7** (210.0 mg, 0.85 mmol) to afford **13** (92.4 mg, 50%) as a brown oil. ¹H NMR (400 MHz, CDCl₃) δ 6.73 (s, 2H), 4.81 (br s, 2H), 3.93 (s, 4H), 3.85 (s, 6H), 2.84–2.81 (m, 2H), 2.76 (m, 2H), 1.76–1.66 (m, 4H). ESI-MS: [M + H]⁺ (m/z = 251.2).

3-(5,6-Dimethoxyisoindolin-2-yl)-propylcarbonylcyclopentadienyl Tricarbonyl Rhenium (20a). Compound **3** (23.0 mg, 0.13 mmol) was added to a solution of **17** (57.7 mg, 0.12 mmol) and KI (20.0 mg, 0.12 mmol) in 5 mL of toluene and 3 mL of triethylamine. The mixture was refluxed at 115 °C for 5 h. After cooling to room temperature, the solvent was evaporated in vacuum. The residue was purified by silica gel chromatography (ethyl acetate/petroleum ether/triethylamine = 1:3:1) to afford **20a** (8.6 mg, 10%) as a dark oil. ¹H NMR (400 MHz, CDCl₃) δ 6.74 (s, 2H), 5.98 (t, J = 2.2 Hz, 2H), 5.37 (t, J = 2.2 Hz, 2H), 3.88 (s, 4H), 3.85 (s, 6H), 2.78–2.71 (m, 4H), 2.00–1.93 (m, 2H). ¹³C NMR (100 MHz, CDCl₃) δ 194.85, 191.91, 148.53, 131.52, 105.99, 96.61, 87.69, 85.11, 59.04, 56.19, 54.98, 36.36, 23.51. HRMS (ESI-ToF), [M + H]⁺: m/z calcd for C₂₂H₂₃NO₆¹⁸⁵Re 582.1055; found 582.1045.

4-(5,6-Dimethoxyisoindolin-2-yl)-butylcarbonylcyclopentadienyl Tricarbonyl Rhenium (21a). The procedure described for the synthesis of **20a** was applied to **18** (70 mg, 0.14 mmol) and **3** (51.9 mg, 0.29 mmol) to afford **21a** as a dark oil (12.8 mg, 10%). ¹H NMR (400 MHz, CDCl₃) δ 6.74 (s, 2H), 5.99 (t, J = 2.3 Hz, 2H), 5.36 (t, J = 2.3 Hz, 2H), 3.94 (s, 4H), 3.85 (s, 6H), 2.79 (t, J = 7.2 Hz, 2H), 2.66 (t, J = 7.0 Hz, 2H), 1.84–1.77 (m, 2H), 1.70–1.62 (m, 2H). ¹³C NMR (100 MHz, CDCl₃) δ 194.74, 191.90, 148.66, 130.90, 105.95, 96.24, 87.82, 85.13, 59.10, 56.19, 55.93, 38.41, 29.70, 27.69, 22.00. HRMS (ESI-ToF), [M + H]⁺: m/z calcd. for C₂₃H₂₅NO₆¹⁸⁵Re 596.1212; found 596.1219.

5-(5,6-Dimethoxyisoindolin-2-yl)-pentylcarbonylcyclopentadienyl Tricarbonyl Rhenium (22a). Compound **3** (31.9 mg, 0.18 mmol) was added to a solution of **19** (60.0 mg, 0.12 mmol), KI (32.1 mg, 0.19 mmol), and K₂CO₃ (25.0 mg, 0.18 mmol) in 10 mL of anhydrous acetonitrile. The mixture was stirred at 90 °C for 5 h. After cooling to room temperature, the mixture was poured with cold water and extracted with CH₂Cl₂. The organic layer was dried over anhydrous MgSO₄, filtered, and concentrated under vacuum. The residue was purified by silica gel chromatography (ethyl acetate/petroleum ether/triethylamine = 1:3:1) to afford **22a** (29.8 mg, 41%) as a dark oil. ¹H NMR (400 MHz, CDCl₃) δ 6.74 (s, 2H), 5.99 (t, J = 2.2 Hz, 2H), 5.39 (t, J = 2.2 Hz, 2H), 3.89 (s, 4H), 3.86 (s, 6H), 2.72 (t, J = 7.4 Hz, 2H), 2.62 (t, J = 7.3 Hz, 2H), 1.78–1.71 (m, 2H), 1.66–1.58 (m, 2H), 1.48–1.42 (m, 2H). ¹³C NMR (125 MHz, CDCl₃) δ 195.20, 191.88, 148.35,

131.71, 105.88, 96.51, 87.90, 85.18, 59.26, 56.13, 55.93, 38.78, 28.72, 26.93, 24.31. HRMS (ESI-ToF), [M + H]⁺: m/z calcd. for C₂₄H₂₇NO₆¹⁸⁵Re 610.1368; found 610.1362.

3-(6,7-Dimethoxy-3,4-dihydro-1H-isoquinolin-2-yl)-propylcarbonylcyclopentadienyl Tricarbonyl Rhenium (23a). The procedure described for the synthesis of **20a** was applied to **17** (53.5 mg, 0.11 mmol) and **4** (32.0 mg, 0.16 mmol) to afford **23a** as a yellow oil (19.7 mg, 30%). ¹H NMR (400 MHz, CDCl₃) δ 6.58 (s, 1H), 6.51 (s, 1H), 5.96 (t, J = 2.2 Hz, 2H), 5.34 (t, J = 2.2 Hz, 2H), 3.84 (s, 3H), 3.83 (s, 3H), 3.56 (s, 2H), 2.81–2.78 (m, 2H), 2.74–2.67 (m, 4H), 2.57 (t, J = 6.8 Hz, 2H), 2.03–1.96 (m, 2H). ¹³C NMR (125 MHz, CDCl₃) δ 194.65, 191.90, 147.99, 147.58, 125.04, 111.31, 109.40, 96.15, 87.84, 85.25, 55.97, 55.95, 54.70, 50.23, 36.29, 29.71, 20.97. HRMS (ESI-ToF), [M + H]⁺: m/z calcd. for C₂₃H₂₅NO₆¹⁸⁵Re 596.1212; found 596.1215.

4-(6,7-Dimethoxy-3,4-dihydro-1H-isoquinolin-2-yl)-butylcarbonylcyclopentadienyl Tricarbonyl Rhenium (24a). The procedure described for the synthesis of **20a** was applied to **18** (60 mg, 0.12 mmol) and **4** (50.1 mg, 0.26 mmol) to afford **24a** as a yellow oil (22 mg, 36%). ¹H NMR (400 MHz, CDCl₃) δ 6.59 (s, 1H), 6.52 (s, 1H), 6.00 (t, J = 2.3 Hz, 2H), 5.33 (t, J = 2.3 Hz, 2H), 3.84 (s, 3H), 3.83 (s, 3H), 3.58 (s, 2H), 2.83 (t, J = 5.2 Hz, 2H), 2.74 (t, J = 5.4 Hz, 2H), 2.65 (t, J = 7.0 Hz, 2H), 2.56 (t, J = 7.0 Hz, 2H), 1.82–1.74 (m, 2H), 1.73–1.63 (m, 2H). ¹³C NMR (100 MHz, CDCl₃) δ 195.10, 191.91, 147.59, 147.28, 126.65, 126.21, 111.46, 109.62, 96.18, 87.94, 85.08, 57.48, 55.96, 55.75, 50.91, 38.58, 29.71, 28.64, 26.29, 22.44. HRMS (ESI-ToF), [M + H]⁺: m/z calcd. for C₂₄H₂₇NO₆¹⁸⁵Re 610.1368; found 610.1366.

5-(6,7-Dimethoxy-3,4-dihydro-1H-isoquinolin-2-yl)-pentylcarbonylcyclopentadienyl Tricarbonyl Rhenium (25a). The procedure described for the synthesis of **22a** was applied to **19** (78.5 mg, 0.15 mmol) and **4** (45.2 mg, 0.23 mmol) to afford **25a** as a colorless oil (48.6 mg, 51%). ¹H NMR (400 MHz, CDCl₃) δ 6.59 (s, 1H), 6.52 (s, 1H), 5.98 (t, J = 2.2 Hz, 2H), 5.38 (t, J = 2.2 Hz, 2H), 3.84 (s, 3H), 3.83 (s, 3H), 3.55 (s, 2H), 2.82 (t, J = 5.7 Hz, 2H), 2.70 (t, J = 5.8 Hz, 2H), 2.61 (t, J = 7.3 Hz, 2H), 2.51 (t, J = 7.5 Hz, 2H), 1.77–1.69 (m, 2H), 1.68–1.59 (m, 2H), 1.45–1.37 (m, 2H). ¹³C NMR (125 MHz, CDCl₃) δ 195.20, 191.88, 147.47, 147.17, 126.73, 126.25, 111.36, 109.50, 96.15, 87.89, 85.18, 58.14, 55.92, 55.91, 55.86, 51.10, 38.79, 28.72, 27.10, 27.04, 24.32. HRMS (ESI-ToF), [M + H]⁺: m/z calcd. for C₂₅H₂₉NO₆¹⁸⁵Re 624.1525; found 624.1519.

2-(5,6-Dimethoxyisoindolin-2-yl)-ethylaminocarbonylcyclopentadienyl Tricarbonyl Rhenium (27a). Under N₂, the solution of compound **11** (60.0 mg, 0.27 mmol) in 1.5 mL of anhydrous DMF and 100 μL of triethylamine was added to the solution of compound **26** (98.2 mg, 0.18 mmol) in 1 mL of anhydrous DMF dropwise. The reaction mixture was stirred at room temperature for 4 h. The solvent was removed, washed with saturated sodium chloride, and extracted with ethyl acetate. The organic layer was dried over anhydrous MgSO₄, filtered, and concentrated under vacuum. The residue was purified by silica gel chromatography (ethyl ether/hexane/triethylamine = 10:5:1) to afford **27a** (49.9 mg, 48%) as a pale yellow solid. Mp: 165.1–167.1 °C. ¹H NMR (400 MHz, CDCl₃) δ 7.16 (br s, 1H), 6.76 (s, 2H), 6.04 (s, 2H), 5.34 (t, J = 2.2 Hz, 2H), 4.12 (s, 4H), 3.87 (s, 6H), 3.61 (q, J = 5.4 Hz, 2H), 3.07 (t, J = 5.3 Hz, 2H). ¹³C NMR (100 MHz, CDCl₃) δ 192.58, 162.28, 148.64, 131.10, 105.93, 95.13, 86.03, 84.66, 58.99, 56.15, 54.36, 38.12. HRMS (ESI-ToF), [M + H]⁺: m/z calcd for C₂₂H₂₁N₂O₆¹⁸⁵Re 583.1008, found 583.0995.

3-(5,6-Dimethoxyisoindolin-2-yl)-propylaminocarbonylcyclopentadienyl Tricarbonyl Rhenium (28a). The procedure described for the synthesis of **27a** was applied to the compound **12** (40.0 mg, 0.17 mmol) and compound **26** (60.0 mg, 0.11 mmol) to afford **28a** (26.1 mg, 40%) as a pale yellow oil. ¹H NMR (400 MHz, CDCl₃) δ 9.05 (br s, 1H), 6.82 (s, 2H), 5.48 (t, J = 2.2 Hz, 2H), 5.10 (t, J = 2.2 Hz, 2H), 3.97 (s, 4H), 3.88 (s, 6H), 3.53 (q, J = 5.4 Hz, 2H), 3.03 (t, J = 5.4 Hz, 2H), 1.84–1.78 (m, 2H). HRMS (ESI-ToF), [M + H]⁺: m/z calcd for C₂₂H₂₄N₂O₆¹⁸⁵Re 597.1164, found 597.1177.

4-(5,6-Dimethoxyisoindolin-2-yl)-butylaminocarbonylcyclopentadienyl Tricarbonyl Rhenium (29a). The procedure described for the synthesis of **27a** was applied to compound **13** (40.0 mg, 0.17 mmol) and compound **26** (81.8 mg, 0.15 mmol) to afford **29a** (34.4 mg, 38%) as a pale yellow oil. ¹H NMR (400 MHz, CDCl₃) δ 8.14 (br s, 1H), 6.78 (s,

2H), 5.57 (t, $J = 2.0$ Hz, 2H), 5.11 (t, $J = 2.2$ Hz, 2H), 3.98 (s, 4H), 3.87 (s, 6H), 3.41 (q, $J = 4.9$ Hz, 2H), 2.85 (t, $J = 5.4$ Hz, 2H), 1.76–1.75 (m, 4H). ^{13}C NMR (100 MHz, CDCl_3) δ 192.95, 162.03, 148.79, 131.16, 106.02, 96.86, 84.99, 84.57, 59.19, 56.17, 55.96, 39.71, 27.71, 26.81. HRMS (ESI-Tof), $[\text{M} + \text{H}]^+$: m/z calcd for $\text{C}_{23}\text{H}_{26}\text{N}_2\text{O}_6^{185}\text{Re}$ 611.1321, found 611.1323.

2-(6,7-Dimethoxy-3,4-dihydroisoquinolin-2(1H)-yl)-ethylamino-carbonylcyclopentadienyl Tricarbonyl Rhenium (30a). The procedure described for the synthesis of 27a was applied to compound 14 (74.4 mg, 0.32 mmol) and compound 26 (85.0 mg, 0.16 mmol) to afford 30a as a light yellow solid (70.4 mg, 74%). Mp: 133.6–134.9 °C. ^1H NMR (400 MHz, CDCl_3) δ 6.62 (s, 1H), 6.53 (s, 1H), 5.96 (s, 2H), 5.33 (t, $J = 2.2$ Hz, 2H), 3.85 (d, $J = 6.3$ Hz, 6H), 3.66 (s, 2H), 3.58 (q, $J = 5.1$ Hz, 2H), 2.90 (s, 4H), 2.81 (s, 2H). ^{13}C NMR (100 MHz, CDCl_3) δ 192.57, 162.19, 147.76, 147.41, 125.89, 125.83, 111.46, 109.54, 95.17, 85.98, 84.66, 56.09, 55.95, 55.93, 55.26, 50.64, 36.32, 28.40, 26.89. HRMS (ESI-Tof), $[\text{M} + \text{H}]^+$: m/z calcd for $\text{C}_{22}\text{H}_{24}\text{N}_2\text{O}_6^{185}\text{Re}$ 597.1164, found 597.1176.

3-(6,7-Dimethoxy-3,4-dihydroisoquinolin-2(1H)-yl)-propylamino-carbonylcyclopentadienyl Tricarbonyl Rhenium (31a). The procedure described for the synthesis of 27a was applied to compound 15 (70.2 mg, 0.28 mmol) and compound 26 (82.7 mg, 0.15 mmol) to afford 31a as a light yellow solid (67.6 mg, 74%). Mp: 123.6–124.5 °C. ^1H NMR (400 MHz, CDCl_3) δ 6.65 (s, 1H), 6.59 (s, 1H), 5.39 (s, 2H), 5.01 (t, $J = 2.0$ Hz, 2H), 3.86 (d, $J = 8.0$ Hz, 6H), 3.66 (s, 2H), 3.51 (q, $J = 5.2$ Hz, 2H), 2.97 (t, $J = 5.8$ Hz, 2H), 2.86 (t, $J = 5.5$ Hz, 2H), 2.79 (t, $J = 5.2$ Hz, 2H), 1.83 (t, $J = 4.7$ Hz, 2H). ^{13}C NMR (100 MHz, CDCl_3) δ 192.94, 161.69, 148.20, 147.62, 126.10, 125.90, 111.44, 109.89, 96.33, 84.93, 84.52, 56.08, 55.96, 55.42, 51.78, 41.31, 28.89, 23.86. HRMS (ESI-Tof), $[\text{M} + \text{H}]^+$: m/z calcd for $\text{C}_{23}\text{H}_{26}\text{N}_2\text{O}_6^{185}\text{Re}$ 611.1321, found 611.1323.

4-(6,7-Dimethoxy-3,4-dihydroisoquinolin-2(1H)-yl)-butylamino-carbonylcyclopentadienyl Tricarbonyl Rhenium (32a). The procedure described for the synthesis of 27a was applied to compound 16 (89.0 mg, 0.34 mmol) and compound 26 (85.9 mg, 0.16 mmol) to afford 32a as a light yellow oil (81.9 mg, 83%). ^1H NMR (400 MHz, CDCl_3) δ 7.55 (br s, 1H), 6.63 (s, 1H), 6.56 (s, 1H), 5.58 (s, 2H), 5.07 (t, $J = 2.2$ Hz, 2H), 3.85 (d, $J = 2.4$ Hz, 6H), 3.65 (s, 2H), 3.41 (q, $J = 5.6$ Hz, 2H), 2.90 (t, $J = 5.8$ Hz, 2H), 2.80 (t, $J = 5.6$ Hz, 2H), 2.63 (t, $J = 6.0$ Hz, 2H), 1.79–1.68 (m, 4H). ^{13}C NMR (100 MHz, CDCl_3) δ 192.92, 161.83, 147.83, 147.40, 126.26, 126.15, 111.49, 109.50, 96.02, 85.46, 84.55, 57.11, 56.66, 55.92, 50.01, 39.22, 28.52, 27.37, 24.69. HRMS (ESI-Tof), $[\text{M} + \text{H}]^+$: m/z calcd for $\text{C}_{24}\text{H}_{28}\text{N}_2\text{O}_6^{185}\text{Re}$ 625.1477, found 625.1483.

3-(5,6-Dimethoxyisoindolin-2-yl)-propylcarbonylferrocene (36). The procedure described for the synthesis of 20a was applied to 33 (97.5 mg, 0.29 mmol) and 3 (75.9 mg, 0.42 mmol) to afford 36 as an orange solid (20.5 mg, 16%). Mp: 116.5–119.4 °C. ^1H NMR (400 MHz, CDCl_3) δ 6.75 (s, 2H), 4.81 (t, $J = 1.7$ Hz, 2H), 4.49 (t, $J = 1.7$ Hz, 2H), 4.20 (s, 5H), 3.94 (s, 4H), 3.86 (s, 6H), 2.88–2.80 (m, 4H), 2.04–1.98 (m, 2H). ESI-MS: $[\text{M} + \text{H}]^+$ ($m/z = 434.6$).

4-(5,6-Dimethoxyisoindolin-2-yl)-butylcarbonylferrocene (37). The procedure described for the synthesis of 20a was applied to 34 (91.3 mg, 0.26 mmol) and 3 (107.5 mg, 0.60 mmol) to afford 37 as an orange solid (25.8 mg, 19%). Mp: 105.6–107.4 °C. ^1H NMR (400 MHz, CDCl_3) δ 6.74 (s, 2H), 4.81 (t, $J = 1.9$ Hz, 2H), 4.49 (t, $J = 1.8$ Hz, 2H), 4.20 (s, 5H), 3.91 (s, 4H), 3.86 (s, 6H), 2.79–2.75 (m, 4H), 1.85–1.78 (m, 2H), 1.71–1.63 (m, 2H). ESI-MS: $[\text{M} + \text{H}]^+$ ($m/z = 447.9$).

5-(5,6-Dimethoxyisoindolin-2-yl)-pentylcarbonylferrocene (38). The procedure described for the synthesis of 22a was applied to 35 (49.3 mg, 0.14 mmol) and 3 (25.1 mg, 0.14 mmol) to afford 38 as an orange solid (56.5 mg, 44%). Mp: 108.1–110.0 °C. ^1H NMR (400 MHz, CDCl_3) δ 6.75 (s, 2H), 4.78 (t, $J = 1.9$ Hz, 2H), 4.49 (t, $J = 1.9$ Hz, 2H), 4.20 (s, 5H), 3.95 (s, 4H), 3.86 (s, 6H), 2.79 (s, 2H), 2.74 (t, $J = 7.4$ Hz, 2H), 1.81–1.73 (m, 2H), 1.69 (s, 2H), 1.53–1.45 (m, 2H). ESI-MS: $[\text{M} + \text{H}]^+$ ($m/z = 462.2$).

3-(6,7-Dimethoxy-3,4-dihydro-1H-isoquinolin-2-yl)-propylcarbonylferrocene (39). The procedure described for the synthesis of 20a was applied to 33 (85.8 mg, 0.26 mmol) and 4 (62.1 mg, 0.32 mmol) to afford 39 as an orange solid (34.3 mg, 33%). Mp: 114.1–116.1 °C. ^1H NMR (400 MHz, CDCl_3) δ 6.60 (s, 1H), 6.53 (s, 1H), 4.79 (t, $J = 1.9$

Hz, 2H), 4.48 (t, $J = 1.9$ Hz, 2H), 4.19 (s, 5H), 3.84 (s, 3H), 3.83 (s, 3H), 3.61 (s, 2H), 2.83 (t, $J = 7.1$ Hz, 2H), 2.77 (s, 2H), 2.63 (s, 2H), 2.04–2.01 (m, 2H). ESI-MS: $[\text{M} + \text{H}]^+$ ($m/z = 448.7$).

4-(6,7-Dimethoxy-3,4-dihydro-1H-isoquinolin-2-yl)-butylcarbonylferrocene (40). The procedure described for the synthesis of 20a was applied to 34 (102.6 mg, 0.29 mmol) and 4 (116.0 mg, 0.60 mmol) to afford 40 as an orange oil (25.7 mg, 22%). ^1H NMR (400 MHz, CDCl_3) δ 6.59 (s, 1H), 6.53 (s, 1H), 4.79 (t, $J = 1.9$ Hz, 2H), 4.49 (t, $J = 1.9$ Hz, 2H), 4.19 (s, 5H), 3.84 (s, 3H), 3.83 (s, 3H), 3.59 (s, 2H), 2.84 (t, $J = 5.6$ Hz, 2H), 2.78–2.73 (m, 4H), 2.57 (t, $J = 7.4$ Hz, 2H), 1.81–1.70 (m, 4H). ESI-MS: $[\text{M} + \text{H}]^+$ ($m/z = 461.9$).

5-(6,7-Dimethoxy-3,4-dihydro-1H-isoquinolin-2-yl)-pentylcarbonylferrocene (41). The procedure described for the synthesis of 22a was applied to 35 (50.3 mg, 0.14 mmol) and 4 (34.1 mg, 0.18 mmol) to afford 41 as an orange solid (152.8 mg, 78%). Mp: 118.6–120.8 °C. ^1H NMR (400 MHz, CDCl_3) δ 6.59 (s, 1H), 6.53 (s, 1H), 4.78 (t, $J = 1.9$ Hz, 2H), 4.49 (t, $J = 1.8$ Hz, 2H), 4.20 (s, 5H), 3.84 (s, 3H), 3.83 (s, 3H), 2.84 (s, 2H), 2.73 (t, $J = 7.4$ Hz, 2H), 2.55 (s, 2H), 1.80–1.72 (m, 2H), 1.68 (s, 2H), 1.49–1.42 (m, 2H). ESI-MS: $[\text{M} + \text{H}]^+$ ($m/z = 476.2$).

4-(5,6-Dimethoxyisoindolin-2-yl)-butylaminocarbonylferrocene (43). Under N_2 , the solution of compound 13 (66.0 mg, 0.26 mmol) in 1.5 mL of anhydrous DMF and 100 μL of triethylamine was added to the solution of compound 42 (102.9 mg, 0.26 mmol) in 1 mL of anhydrous DMF dropwise. The reaction mixture was stirred at room temperature for 4 h. The solvent was removed, then washed with saturated sodium chloride, and extracted with ethyl acetate. The organic layer was dried over anhydrous MgSO_4 , filtered, and concentrated under vacuum. The residue was purified by silica gel chromatography (ethyl ether/hexane/triethylamine = 10:5:1) to afford 43 (78.4 mg, 65%) as a yellow solid. Mp: 119.6–120.4 °C. ^1H NMR (400 MHz, CDCl_3) δ 6.76 (s, 2H), 6.62 (br s, 1H), 4.61 (s, 2H), 4.25 (s, 2H), 4.16 (s, 5H), 4.00 (s, 4H), 3.87 (s, 6H), 3.44 (d, $J = 5.4$ Hz, 2H), 2.86 (s, 2H), 1.74–1.70 (m, 4H). ^{13}C NMR (100 MHz, CDCl_3) δ 170.12, 148.68, 131.14, 130.90, 105.99, 70.13, 69.67, 68.07, 65.55, 59.20, 56.20, 55.62, 39.33, 27.72, 26.33. HRMS (EI): m/z calcd for $\text{C}_{25}\text{H}_{31}\text{N}_2\text{O}_3\text{Fe}$ $[\text{M} + \text{H}]^+$ 463.1684, found 463.1686.

2-(6,7-Dimethoxy-3,4-dihydroisoquinolin-2(1H)-yl)-ethylamino-carbonylferrocene (44). The procedure described for the synthesis of 43 was applied to compound 14 (38.0 mg, 0.16 mmol) and compound 42 (53.8 mg, 0.14 mmol) to afford 44 (49.8 mg, 69%) as a light yellow solid. Mp: 193.9–195.1 °C. ^1H NMR (400 MHz, CDCl_3) δ 6.62 (s, 1H), 6.55 (s, 1H), 6.48 (br s, 1H), 4.66 (s, 2H), 4.30 (t, $J = 1.8$ Hz, 2H), 4.15 (s, 5H), 3.84 (d, $J = 9.8$ Hz, 6H), 3.68 (s, 2H), 3.59 (q, $J = 5.4$ Hz, 2H), 2.89–2.84 (m, 4H), 2.78 (t, $J = 5.6$ Hz, 2H). ^{13}C NMR (100 MHz, CDCl_3) δ 170.35, 147.68, 147.38, 126.12, 125.99, 111.43, 109.47, 70.24, 69.68, 68.18, 56.64, 55.96, 55.94, 55.36, 50.91, 36.19, 28.71. HRMS (EI): m/z calcd for $\text{C}_{24}\text{H}_{29}\text{N}_2\text{O}_3\text{Fe}$ $[\text{M} + \text{H}]^+$ 449.1528, found 449.1520.

3-(6,7-Dimethoxy-3,4-dihydroisoquinolin-2(1H)-yl)-propylamino-carbonylferrocene (45). The procedure described for the synthesis of 43 was applied to compound 15 (100.0 mg, 0.40 mmol) and compound 42 (158.4 mg, 0.40 mmol) to afford 45 (116.6 mg, 63%) as an orange solid. Mp: 72.2–73.6 °C. ^1H NMR (400 MHz, CDCl_3) δ 7.73 (br s, 1H), 6.66 (s, 1H), 6.57 (s, 1H), 4.40 (s, 2H), 4.10 (s, 2H), 4.09 (s, 5H), 3.89 (s, 3H), 3.84 (s, 3H), 3.68 (s, 2H), 3.53 (q, $J = 5.4$ Hz, 2H), 2.94 (t, $J = 5.9$ Hz, 2H), 2.86–2.84 (m, 2H), 2.77 (t, $J = 5.6$ Hz, 2H), 1.89–1.84 (m, 2H). ^{13}C NMR (100 MHz, CDCl_3) δ 170.02, 147.88, 147.42, 126.36, 126.04, 111.43, 109.62, 69.99, 69.54, 67.86, 58.13, 56.04, 55.94, 55.79, 51.54, 40.32, 28.83, 25.19. ESI-MS: $[\text{M} + \text{H}]^+$ ($m/z = 462.8$).

4-(6,7-Dimethoxy-3,4-dihydroisoquinolin-2(1H)-yl)-butylamino-carbonylferrocene (46). The procedure described for the synthesis of 43 was applied to compound 16 (36.7 mg, 0.14 mmol) and compound 42 (63.0 mg, 0.16 mmol) to afford 46 (45.0 mg, 68%) as an orange solid. Mp: 86.3–87.8 °C. ^1H NMR (400 MHz, CDCl_3) δ 6.61 (s, 1H), 6.52 (s, 1H), 4.59 (s, 2H), 4.25 (t, $J = 1.8$ Hz, 2H), 4.17 (s, 5H), 3.84 (d, $J = 9.8$ Hz, 6H), 3.62 (s, 2H), 3.43 (q, $J = 6.2$ Hz, 2H), 2.87 (d, $J = 5.4$ Hz, 2H), 2.79 (d, $J = 5.1$ Hz, 2H), 2.61 (t, $J = 6.1$ Hz, 2H), 1.76–1.68 (m, 4H). ^{13}C NMR (100 MHz, CDCl_3) δ 170.04, 147.64, 147.29, 126.46, 126.17, 111.42, 109.56, 70.17, 69.66, 68.03, 57.52, 56.03, 55.94, 50.76, 39.31, 28.60, 27.79, 24.69. HRMS (ESI-Tof), $[\text{M} + \text{H}]^+$: m/z calcd for $\text{C}_{26}\text{H}_{33}\text{N}_2\text{O}_3\text{Fe}$ 477.1841, found 477.1833.

X-ray Crystallography. All of the procedures for X-ray crystallography were previously described.³⁶ Detailed procedures are described in the [Supporting Information](#).

In Vitro Radioligand Competition Studies. σ Receptor Binding Assays. All of the procedures for the radioligand competition studies were previously described.²⁰ Detailed procedures are described in the [Supporting Information](#).

VACHT Binding Assays. The determination of the affinity for VACHT were conducted by a method in the literature.³⁸ Detailed procedures are described in the [Supporting Information](#).

Dopamine D_{2L} Receptors, NMDA Receptors, Opiate Receptors, DAT, NET, and SERT Binding Assay. The affinities of compound **20a** for the above receptors and transporters are presented in a percentage of inhibition form. Detailed information is described in the [Supporting Information](#).

Radiochemistry. ^{99m}Tc-pertechnetate was eluted from a commercial ⁹⁹Mo–^{99m}Tc generator obtained from Beijing Atomic High-tech Co. The reactions were performed according to the methods in the literature.^{22,25,39} Detailed procedures are provided in the [Supporting Information](#).

Measurement of log D values. The log D values of [^{99m}Tc]**20b**–**25b** and [^{99m}Tc]**29b**–**30b** were determined by measuring the distribution of the radiotracer between 1-octanol and 0.05 M sodium phosphate buffer at pH 7.4 according to the literature.^{22,25,36} Detailed procedures are provided in the [Supporting Information](#).

In Vitro Evaluation in DU145 Prostate Cells and C6 Glioma Cells. The culture of cells and the *in vitro* cell uptake and blocking assays were performed as previously reported.^{22,25} Detailed procedures are provided in the [Supporting Information](#).

Biodistribution and Blocking Studies in Mice. All animal experiments in ICR mice (*n* = 5, 4–5 weeks, 22–25 g) were performed in compliance with the national laws related to the care and experiments on laboratory animals. Biodistribution studies and blocking studies of HPLC-purified [^{99m}Tc]**20b**, [^{99m}Tc]**23b**, [^{99m}Tc]**25b**, and [^{99m}Tc]**29b** (370 kBq, 0.1 mL) were carried out based on a method reported previously.^{22,25} Detailed procedures are provided in the [Supporting Information](#).

Biodistribution and Blocking Studies of [^{99m}Tc]20b** in Balb/c Nude Mice Bearing C6 Glioma Xenografts.** All animal experiments in Balb/c nude mice (*n* = 4) were performed in compliance with the national laws related to the care and experiments on laboratory animals. Biodistribution studies and blocking studies of [^{99m}Tc]**20b** (370 kBq, 0.1 mL) were carried out based on a method reported previously.²⁵ Detailed procedures are provided in the [Supporting Information](#).

Small Animal NanoScan SPECT/CT Imaging of [^{99m}Tc]20b**.** The detailed procedures of small animal imaging studies of [^{99m}Tc]**20b** (22.2 MBq, 0.15 mL) in male Balb/c nude mice bearing C6 glioma xenografts are provided in the [Supporting Information](#).

In Vivo Radiometabolic Stability of [^{99m}Tc]20b**.** The *in vivo* metabolism of [^{99m}Tc]**20b** (18.5 MBq, 0.15 mL) was studied in male ICR mice according to a previously reported method.³⁶ Detailed procedures are provided in the [Supporting Information](#).

■ ASSOCIATED CONTENT

■ Supporting Information

The Supporting Information is available free of charge on the ACS Publications website at DOI: [10.1021/acs.jmedchem.5b01378](https://doi.org/10.1021/acs.jmedchem.5b01378).

General information and some parts of the evaluation of the radiotracers in [Experimental Section](#), purity of key target compounds, the HPLC chromatograms of **20a**–**25a** and [^{99m}Tc]**20b**–**25b**, **29a**–**30a**, and [^{99m}Tc]**29b**–**30b**, X-ray crystallographic data for compound **31a**, *in vitro* evaluation of [^{99m}Tc]**21b** and [^{99m}Tc]**24b** in C6 glioma tumor cell line, biodistribution and blocking studies of [^{99m}Tc]**25b** in male ICR mice, small animal NanoScan SPECT/CT imaging of [^{99m}Tc]**20b** ([PDF](#))

Crystal information file of compound **31a** ([CIF](#))

SMILES data ([CSV](#))

■ AUTHOR INFORMATION

Corresponding Author

*Phone: +86-10-58808891. Fax: +86-10-58808891. E-mail: hmjia@bnu.edu.cn.

Author Contributions

[†]D.L. and Y.C. contributed equally to this work.

Notes

The authors declare no competing financial interest.

■ ACKNOWLEDGMENTS

We give special thanks to Professor Robert H. Mach for his helpful suggestions and valuable comments on this manuscript. We are grateful to Dr. Xuebing Deng (College of Chemistry, Beijing Normal University) for his assistance with X-ray diffraction. This work was supported by the National Natural Science Foundation of China (No. 21471019).

■ ABBREVIATIONS USED

CNS, central nervous system; DAT, dopamine transporter; DLT, double ligand transfer; DMF, dimethylformamide; DTG, 1,3-di-*o*-tolyl-guanidine; [¹⁸F]ISO-1, *N*-(4-(6,7-dimethoxy-3,4-dihydroisoquinolin-2(1*H*)-yl)butyl)-2-(2-¹⁸F)fluoroethoxy)-5-methylbenzamide; FBS, fetal bovine serum; BBB, blood–brain barrier; HPLC, high performance liquid chromatography; ID, injected dose; NET, norepinephrine transporter; PET, positron emission tomography; rt, room temperature; SD, standard deviation; SERT, serotonin transporter; SPECT, single photon emission computed tomography; TFA, trifluoroacetic acid; THF, tetrahydrofuran; TLC, thin layer chromatography; VACHT, vesicular acetylcholine transporter

■ REFERENCES

- (1) Bading, J. R.; Shields, A. F. Imaging of cell proliferation: status and prospects. *J. Nucl. Med.* **2008**, *49*, 64S–80S.
- (2) Bem, W. T.; Thomas, G. E.; Mamone, J. Y.; Homan, S. M.; Levy, B. K.; Johnson, F. E.; Coscia, C. J. Overexpression of σ receptors in nonneural human tumors. *Cancer Res.* **1991**, *51*, 6558–6562.
- (3) Vilner, B. J.; John, C. S.; Bowen, W. D. Sigma-1 and sigma-2 receptors are expressed in a wide variety of human and rodent tumor cell lines. *Cancer Res.* **1995**, *55*, 408–413.
- (4) John, C. S.; Vilner, B. J.; Geyer, B. C.; Moody, T.; Bowen, W. D. Targeting sigma receptor-binding benzamides as *in vivo* diagnostic and therapeutic agents for human prostate tumors. *Cancer Res.* **1999**, *59*, 4578–4583.
- (5) van Waarde, A.; Rybczynska, A. A.; Ramakrishnan, N. K.; Ishiwata, K.; Elsinga, P. H.; Dierckx, R. A. J. O. Sigma receptors in oncology: therapeutic and diagnostic applications of sigma ligands. *Curr. Pharm. Des.* **2010**, *16*, 3519–3537.
- (6) Megalizzi, V.; Le Mercier, M.; Decaestecker, C. Sigma receptors and their ligands in cancer biology: overview and new perspectives for cancer therapy. *Med. Res. Rev.* **2012**, *32*, 410–427.
- (7) Mach, R. H.; Smith, C. R.; Al-Nabulsi, I.; Whirrett, B. R.; Childers, S. R.; Wheeler, K. T. σ_2 receptors as potential biomarkers of proliferation in breast cancer. *Cancer Res.* **1997**, *57*, 156–161.
- (8) Al-Nabulsi, I.; Mach, R. H.; Wang, L. M.; Wallen, C. A.; Keng, P. C.; Sten, K.; Childers, S. R.; Wheeler, K. T. Effect of ploidy, recruitment, environmental factors, and tamoxifen treatment on the expression of sigma-2 receptors in proliferating and quiescent tumour cells. *Br. J. Cancer* **1999**, *81*, 925–933.
- (9) Wheeler, K. T.; Wang, L. M.; Wallen, C. A.; Childers, S. R.; Cline, J. M.; Keng, P. C.; Mach, R. H. Sigma-2 receptors as a biomarker of proliferation in solid tumours. *Br. J. Cancer* **2000**, *82*, 1223–1232.

- (10) Tu, Z.; Xu, J.; Jones, L. A.; Li, S.; Dumstorff, C.; Vangveravong, S.; Chen, D. L.; Wheeler, K. T.; Welch, M. J.; Mach, R. H. Fluorine-18-labeled benzamide analogues for imaging the σ_2 receptor status of solid tumors with Positron Emission Tomography. *J. Med. Chem.* **2007**, *50*, 3194–3204.
- (11) Dehdashti, F.; Laforest, R.; Gao, F.; Shoghi, K. I.; Aft, R. L.; Nussenbaum, B.; Kreisel, F. H.; Bartlett, N. L.; Cashen, A.; Wagner-Johnson, N.; Mach, R. H. Assessment of cellular proliferation in tumors by PET using ^{18}F -ISO-1. *J. Nucl. Med.* **2013**, *54*, 350–357.
- (12) Shoghi, K. I.; Xu, J.; Su, Y.; He, J.; Rowland, D.; Yan, Y.; Garbow, J. R.; Tu, Z.; Jones, L. A.; Higashikubo, R.; Wheeler, K. T.; Lubet, R. A.; Mach, R. H.; You, M. Quantitative receptor-based imaging of tumor proliferation with the sigma-2 ligand [^{18}F]ISO-1. *PLoS One* **2013**, *8*, e74188.
- (13) Mach, R. H.; Wheeler, K. T. Development of molecular probes for imaging sigma-2 receptors in vitro and in vivo. *Cent. Nerv. Syst. Agents Med. Chem.* **2009**, *9*, 230–245.
- (14) Sai, K. K. S.; Jones, L. A.; Mach, R. H. Development of ^{18}F -labeled PET probes for imaging cell proliferation. *Curr. Top. Med. Chem.* **2013**, *13*, 892–908.
- (15) Mach, R. H.; Zeng, C.; Hawkins, W. G. The σ_2 receptor: a novel protein for the imaging and treatment of cancer. *J. Med. Chem.* **2013**, *56*, 7137–7160.
- (16) Bailey, D. L.; Willowson, K. P. An evidence-based review of quantitative SPECT imaging and potential clinical applications. *J. Nucl. Med.* **2013**, *54*, 83–98.
- (17) John, C. S.; Lim, B. B.; Geyer, B. C.; Vilner, B. J.; Bowen, W. D. $^{99\text{m}}\text{Tc}$ -labeled σ -receptor-binding complex: synthesis, characterization, and specific binding to human ductal breast carcinoma (T47D) cells. *Bioconjugate Chem.* **1997**, *8*, 304–309.
- (18) Choi, S. R.; Yang, B.; Plössl, K.; Chumpradit, S.; Wey, S. P.; Acton, P. D.; Wheeler, K.; Mach, R. H.; Kung, H. F. Development of a Tc-99m labeled sigma-2 receptor-specific ligand as a potential breast tumor imaging agent. *Nucl. Med. Biol.* **2001**, *28*, 657–666.
- (19) Friebe, M.; Mahmood, A.; Bolzati, C.; Drews, A.; Johannsen, B.; Eisenhut, M.; Kraemer, D.; Davison, A.; Jones, A. G. [$^{99\text{m}}\text{Tc}$]-Oxotechnetium(V) complexes of amine-amide-dithiol chelates with dialkylaminoalkyl substituents as potential diagnostic probes for malignant melanoma. *J. Med. Chem.* **2001**, *44*, 3132–3140.
- (20) Fan, C.; Jia, H.; Deuther-Conrad, W.; Brust, P.; Steinbach, J.; Liu, B. Novel $^{99\text{m}}\text{Tc}$ labeled σ receptor ligand as a potential tumor imaging agent. *Sci. China, Ser. B: Chem.* **2006**, *49*, 169–176.
- (21) Lu, J.; Kong, D.; Jia, H.; Deuther-Conrad, W.; Brust, P.; Wang, X. Preparation and biological evaluation of $^{99\text{m}}\text{TcN-4}$ -(cyclohexylpiperazin-1-yl)dithioformate as a potential sigma receptor imaging agent. *J. Labelled Compd. Radiopharm.* **2007**, *50*, 1200–1205.
- (22) Chen, X.; Cui, M. C.; Deuther-Conrad, W.; Tu, Y. F.; Ma, T.; Xie, Y.; Jia, B.; Li, Y.; Xie, F.; Wang, X.; Steinbach, J.; Brust, P.; Liu, B. L.; Jia, H. M. Synthesis and biological evaluation of a novel $^{99\text{m}}\text{Tc}$ cyclopentadienyl tricarbonyl complex $[(\text{Cp-R})^{99\text{m}}\text{Tc}(\text{CO})_3]$ for sigma-2 receptor tumor imaging. *Bioorg. Med. Chem. Lett.* **2012**, *22*, 6352–6357.
- (23) Xie, F.; Kniess, T.; Neuber, C.; Deuther-Conrad, W.; Mamat, C.; Lieberman, B. P.; Liu, B.; Mach, R. H.; Brust, P.; Steinbach, J.; Pietzsch, J.; Jia, H. Novel indole-based sigma-2 receptor ligands: synthesis, structure-affinity relationship and antiproliferative activity. *MedChem-Comm* **2015**, *6*, 1093–1103.
- (24) Fan, K. H.; Lever, J. R.; Lever, S. Z. Effect of structural modification in the amine portion of substituted aminobutyl-benzamides as ligands for binding σ_1 and σ_2 receptors. *Bioorg. Med. Chem.* **2011**, *19*, 1852–1859.
- (25) Wang, X.; Li, D.; Deuther-Conrad, W.; Lu, J.; Xie, Y.; Jia, B.; Cui, M.; Steinbach, J.; Brust, P.; Liu, B.; Jia, H. Novel cyclopentadienyl tricarbonyl $^{99\text{m}}\text{Tc}$ complexes containing 1-piperonylpiperazine moiety: potential imaging probes for sigma-1 receptors. *J. Med. Chem.* **2014**, *57*, 7113–7125.
- (26) Shumway, S. D.; Toniatti, C.; Roberts, B. S.; Martin, M. M. Compositions and Methods for Treating Cancer. WO2013039854A1, 2013.
- (27) Mach, R. H.; Huang, Y.; Freeman, R. A.; Wu, L.; Vangveravong, S.; Luedtke, R. R. Conformationally-flexible benzamide analogues as dopamine D_3 and σ_2 receptor ligands. *Bioorg. Med. Chem. Lett.* **2004**, *14*, 195–202.
- (28) Peindy N'Dongo, H. W.; Liu, Y.; Can, D.; Schmutz, P.; Spingler, B.; Alberto, R. Aqueous syntheses of $[(\text{Cp-R})\text{M}(\text{CO})_3]$ type complexes (Cp = cyclopentadienyl, M = Mn, $^{99\text{m}}\text{Tc}$, Re) with bioactive functionalities. *J. Organomet. Chem.* **2009**, *694*, 981–987.
- (29) Li, D.; Wang, X.; Deuther-Conrad, W.; Chen, X.; Cui, M. C.; Steinbach, J.; Brust, P.; Liu, B.; Jia, H. Synthesis and preliminary evaluation of novel $[(\text{Cp-R})\text{M}(\text{CO})_3]$ (M = Re, $^{99\text{m}}\text{Tc}$) complexes as potent sigma-2 receptor ligands. *J. Labelled. Compd. Radiopharm.* **2013**, *56*, S383.
- (30) Chen, Y.; Deuther-Conrad, W.; Steinbach, J.; Brust, P.; Liu, B.; Jia, H. A novel cyclopentadienyl tricarbonyl $^{99\text{m}}\text{Tc}$ complex containing 5,6-dimethoxyisindoline motif – synthesis and evaluation of a radiotracer for imaging of sigma-2 receptors in cancer. *J. Labelled. Compd. Radiopharm.* **2015**, *58*, S98.
- (31) Perregaard, J.; Moltzen, E. K.; Meier, E.; Sanchez, C. Sigma ligands with subnanomolar affinity and preference for the sigma 2 binding site. 1. 3-(omega-aminoalkyl)-1H-indoles. *J. Med. Chem.* **1995**, *38*, 1998–2008.
- (32) Niso, M.; Abate, C.; Contino, M.; Ferorelli, S.; Azzariti, A.; Perrone, R.; Colabufo, N. A.; Berardi, F. Sigma-2 receptor agonists as possible antitumor agents in resistant tumors: hints for collateral sensitivity. *ChemMedChem* **2013**, *8*, 2026–2035.
- (33) Wang, X.; Li, Y.; Deuther-Conrad, W.; Xie, F.; Chen, X.; Cui, M.-C.; Zhang, X.-J.; Zhang, J.-M.; Steinbach, J.; Brust, P.; Liu, B.-L.; Jia, H.-M. Synthesis and biological evaluation of ^{18}F labeled fluoro-oligo-ethoxylated 4-benzylpiperazine derivatives for sigma-1 receptor imaging. *Bioorg. Med. Chem.* **2013**, *21*, 215–222.
- (34) Laruelle, M.; Slifstein, M.; Huang, Y. Relationships between radiotracer properties and image quality in molecular imaging of the brain with positron emission tomography. *Mol. Imaging Biol.* **2003**, *5*, 363–75.
- (35) Huang, Y.; Zheng, M.-Q.; Gerdes, J. M. Development of effective PET and SPECT imaging agents for the serotonin transporter: has a twenty-year journey reached its destination? *Curr. Top. Med. Chem.* **2010**, *10*, 1499–1526.
- (36) Li, Y.; Wang, X.; Zhang, J.; Deuther-Conrad, W.; Xie, F.; Zhang, X.; Liu, J.; Qiao, J.; Cui, M.; Steinbach, J.; Brust, P.; Liu, B.; Jia, H. Synthesis and evaluation of novel ^{18}F -labeled spirocyclic piperidine derivatives as σ_1 receptor ligands for positron emission tomography imaging. *J. Med. Chem.* **2013**, *56*, 3478–3491.
- (37) Glennon, R. A. Binding characteristics of σ_2 receptor ligands. *Rev. Bras. Cienc. Farm.* **2005**, *41*, 1–12.
- (38) Sorger, D.; Scheunemann, M.; Grossmann, U.; Fischer, S.; Vercouille, J.; Hiller, A.; Wenzel, B.; Roghani, A.; Schliebs, R.; Brust, P.; Sabri, O.; Steinbach, J. A new ^{18}F -labeled fluoroacetylmorpholino derivative of vesamicol for neuroimaging of the vesicular acetylcholine transporter. *Nucl. Med. Biol.* **2008**, *35*, 185–195.
- (39) Saidi, M.; Kothari, K.; Pillai, M. R. A.; Hassan, A.; Sarma, H. D.; Chaudhari, P. R.; Unnikrishnan, T. P.; Korde, A.; Azzouz, Z. Cyclopentadienyl technetium ($^{99\text{m}}\text{Tc}$) tricarbonyl piperidine conjugates: biodistribution and imaging studies. *J. Labelled Compd. Radiopharm.* **2001**, *44*, 603–618.